DIPARTIMENTO DI INFORMATICA
E SISTEMISTICA ANTONIO RUBERTI

SAPIENZA
UNIVERSITÀ DI ROMA

Dynamic Gravity Cancellation and Regulation Control in Robots with Flexible Transmissions: Constant, Nonlinear, and Variable Stiffness

Alessandro De Luca
Fabrizio Flacco

Technical Report n. 11, 2010

Dynamic Gravity Cancellation and Regulation Control in Robots with Flexible Transmissions: Constant, Nonlinear, and Variable Stiffness

Alessandro De Luca Fabrizio Flacco

Dipartimento di Informatica e Sistemistica
Università di Roma "La Sapienza"
Via Ariosto 25, 00185 Roma, Italy
{deluca,fflacco}@dis.uniroma1.it

July 2, 2010

Abstract

We consider the problem of perfect cancellation of gravity effects in the dynamics of robot manipulators having flexible transmissions at the joints. Based on the feedback equivalence principle, we aim at designing feedback control laws that let the system outputs behave as those of the same robot device when gravity is absent. The cases of constant stiffness (elastic joints), nonlinear flexible, and variable nonlinear flexible transmissions with antagonistic actuation are analyzed. As a particular case, antagonistic actuation with transmissions having constant but different stiffness is also considered. In all these situations, viable solutions are obtained either in closed algebraic form or by a simple numerical technique. The compensated system can then be controlled without taking into account the gravity bias, which is particularly relevant for safe physical human-robot interaction tasks where such compliant manipulators are commonly used. Moreover, dynamic gravity cancellation allows to design new PD-type regulation controllers and to show their global asymptotic stability without the need of any positive lower bound neither on the stiffness nor on the proportional control gain. A Lyapunov-based proof is provided for the case of robots with elastic joints. Simulation results are reported to illustrate the obtained performance in the various robotic systems with flexible transmissions.

Keywords: robots with flexible joints, variable stiffness actuation, feedback equivalence, gravity cancellation, motion and stiffness control.

1 Introduction

Robots in physical interaction with humans are conveniently controlled so as to achieve zero-gravity operation [1]. This avoids biasing the robot reaction to unintended collisions along the gradient of the gravitational potential, with a uniform and more predictable (thus safer) robot behavior in its whole workspace [2]. Perfect cancellation of gravity is trivial for fully rigid manipulators. In fact, for their standard dynamic model

$$\boldsymbol{M}(\boldsymbol{q})\ddot{\boldsymbol{q}} + \boldsymbol{c}(\boldsymbol{q},\dot{\boldsymbol{q}}) + \boldsymbol{g}(\boldsymbol{q}) = \boldsymbol{\tau},$$

the choice

$$\boldsymbol{\tau} = \boldsymbol{\tau}_g + \boldsymbol{\tau}_0, \qquad \boldsymbol{\tau}_g = \boldsymbol{g}(\boldsymbol{q})$$

removes gravity from the picture in a complete way (i.e., both statically and dynamically), thanks to the colocation of gravity and input torques (and to the full actuation of the system). The additional command $\boldsymbol{\tau}_0$ is left to the control designer for performing desired tasks, e.g., set-point regulation, trajectory tracking, or reaction to a contact with the environment.

However, robots intended for physical Human-Robot Interaction (pHRI) include compliant elements in their mechanical construction, in order to reduce the possibility of injuries due to unexpected collisions [3]. Robot links are designed as lightweight but rigid, while compliance is typically concentrated in the transmissions at the joints, either with finite constant stiffness $\boldsymbol{K}$, e.g., when using harmonic drives [4], or with variable (and independently actuated) nonlinear stiffness [5].

The common dynamic model of robots with constant joint elasticity takes the form [6]

$$\begin{aligned} \boldsymbol{M}(\boldsymbol{q})\ddot{\boldsymbol{q}} + \boldsymbol{c}(\boldsymbol{q},\dot{\boldsymbol{q}}) + \boldsymbol{g}(\boldsymbol{q}) + \boldsymbol{K}(\boldsymbol{q}-\boldsymbol{\theta}) &= \boldsymbol{0} \\ \boldsymbol{B}\ddot{\boldsymbol{\theta}} + \boldsymbol{K}(\boldsymbol{\theta}-\boldsymbol{q}) &= \boldsymbol{\tau}, \end{aligned}$$

where actuation torques $\boldsymbol{\tau}$ appear on the motor side of the elastic joints (i.e., performing work on $\boldsymbol{\theta}$), while gravity loading $\boldsymbol{g}(\boldsymbol{q})$ affects primarily the dynamic behavior of the variables on the link side (i.e., $\boldsymbol{q}$). This non-colocation is a major problem for control. Gravity compensation laws have been proposed for regulation tasks, when the link position $\boldsymbol{q}$ has to be asympotically stabilized to a desired constant value $\boldsymbol{q}_d$. A first solution is based on motor PD feedback with *constant* gravity compensation at steady state [7]

$$\boldsymbol{\tau}_0 = \boldsymbol{K}_P(\boldsymbol{\theta}_d - \boldsymbol{\theta}) - \boldsymbol{K}_D\dot{\boldsymbol{\theta}}, \qquad \boldsymbol{\tau}_g = \boldsymbol{g}(\boldsymbol{q}_d),$$

with $\boldsymbol{\theta}_d = \boldsymbol{q}_d + \boldsymbol{K}^{-1}\boldsymbol{g}(\boldsymbol{q}_d)$, $\boldsymbol{K}_P > 0$, and $\boldsymbol{K}_D > 0$. In order to show asympotic stability by Lyapunov arguments, the proportional gain should be chosen so that the norm of $\boldsymbol{K}_P$ is larger than a positive constant related to gravity, whereas the stiffness matrix $\boldsymbol{K}$ is assumed to dominate the gradient of $\boldsymbol{g}(\boldsymbol{q})$. Indeed, this compensation cancels gravity only in the final *static* condition. Since the gravity term

changes with the robot configuration, an *on-line* compensation has been proposed in [8] by evaluating $\boldsymbol{g}$ in $\boldsymbol{\tau}_g$ with a gravity-biased measure of the motor position

$$\boldsymbol{\tau}_g = \boldsymbol{g}(\tilde{\boldsymbol{\theta}}), \qquad \tilde{\boldsymbol{\theta}} = \boldsymbol{\theta} - \boldsymbol{K}^{-1}\boldsymbol{g}(\boldsymbol{q}_d).$$

While the transient performance is largely improved, the theoretical restriction on $\boldsymbol{K}_P$ could not be removed in the Lyapunov analysis. A better result is achieved in [9], with a gravity compensation of the form

$$\boldsymbol{\tau}_g = \boldsymbol{g}(\bar{\boldsymbol{q}}(\boldsymbol{\theta})),$$

where, for a measured motor position $\boldsymbol{\theta}$, $\bar{\boldsymbol{q}}(\boldsymbol{\theta})$ is computed by numerically solving the *quasi-static* relation $\boldsymbol{g}(\boldsymbol{q}) + \boldsymbol{K}(\boldsymbol{q} - \boldsymbol{\theta}) = \boldsymbol{0}$. This variant is able to relax the lower bound on $\boldsymbol{K}_P$ so that asymptotic stability can be shown through a modified Lyapunov function. On the other hand, the structural condition on the joint stiffness $\|\boldsymbol{K}\| > \|\partial \boldsymbol{g}(\boldsymbol{q})/\partial \boldsymbol{q}\|$ should still hold.

All the above control laws have the merit of using only feedback from the motor variables $\boldsymbol{\theta}$ and $\dot{\boldsymbol{\theta}}$. However, none of them removes completely the effects of gravity, especially in highly *dynamic* tasks: only a partial compensation, and not a cancellation, of the gravitational load acting on the robot link motion is obtained. In the context of robot reaction to collisions, we also note that a practical solution for compensating gravity in elastic joint robots has been proposed in [10], based on the availability of joint torque sensors. The use of this additional sensor can be interpreted as involving also the link position $\boldsymbol{q}$ in the control law. Furthermore, under the assumption that full state is available, it is known that all robots with elastic joints can be exactly linearized by means of a static [11] or dynamic state feedback (the latter is needed when some extra inertial terms are included in the model) [12]. This structural control property will be further exploited in this paper.

The most recent research in pHRI calls for the use of *variable stiffness actuation* (VSA), in which each joint is driven by two independent actuators that allow to control link motion as well as device stiffness [13, 14, 15, 16] and to shape the compliant interaction with the environment. Actuators are typically arranged in *antagonistic* mode [17], with both motors of each joint being involved in robot motion and stiffness variation. Other systems use a separate actuation [18, 19] for stiffness control. In any event, in order to modify the device stiffness, a nonlinear characteristics of the flexible transmissions is needed. This can be realized using either nonlinear springs or linear springs mounted on nonlinear kinematic mechanisms. For VSA systems, the paradigm is "design for safety, control for performance" [5]. In particular, the robot can be made more compliant at high speeds and stiffer at low speeds, thus limiting the energy exchange in the first few instants after an unexpected impact. Up to now, the presence of gravity in VSA-based robots has not been treated rigorously, with experimental single-dof devices moving in the horizontal plane or using only a partial gravity compensation —just as in the constant stiffness case. Nonetheless, a large class of VSA-based systems of the antagonistic type has been shown to be feedback equivalent to linear, controllable,

and input-output decoupled systems [20,21], with the linearizing outputs being the link position and the device stiffness. Also for this class of flexible devices, such a control property will be useful for removing the dynamic effects of gravity in a complete and efficient way.

In this paper, we present new control results that allow perfect gravity cancellation for a variety of robotic systems with flexible transmissions. Based on the general principle of feedback equivalence [22], we will design for all cases static state feedback laws that accurately match the same dynamic behavior of the driven links as if they were moving in the absence of gravity. In Sect. 2, we consider the case of robots with n elastic joints having constant stiffness and single actuation. To illustrate one of the benefits of this approach, Section 3 presents and analyzes a global PD-type regulation controller for robots with elastic joints, which is designed on top of the available dynamic gravity cancellation law. An interesting outcome is that there are no restrictions imposed by gravity neither on the control gains nor on the joint stiffness. In Sect. 4, the design of a dynamic gravity cancellation law is extended to transmissions with nonlinear flexibility and single actuation. The case of double antagonistic actuation with variable nonlinear stiffness is handled in Sect. 5. For VSA-based robots, we will be able to impose also a dynamic behavior to the nonlinear stiffness of the device which is identical to that of the no-gravity case. Finally, the particular instance of antagonistic actuation with transmissions having constant but different stiffness is considered in Sect. 6. In this case, the actuation becomes redundant for motion purposes and space is left for optimizing the control torques. Illustrative simulation results are given in each section.

2 Robots with Elastic Joints

Consider a robot manipulator having n elastic joints of constant stiffness and with n driving motors. Let $\boldsymbol{q}$ and $\boldsymbol{\theta}$ be the n-dimensional vectors of link and motor variables. Under the simplifying modeling assumption of Spong [11], and including also viscous effects at the motor and link side, the dynamic model takes the form

$$\boldsymbol{M}(\boldsymbol{q})\ddot{\boldsymbol{q}} + \boldsymbol{c}(\boldsymbol{q},\dot{\boldsymbol{q}}) + \boldsymbol{g}(\boldsymbol{q}) + \boldsymbol{D}_q\dot{\boldsymbol{q}} + \boldsymbol{K}(\boldsymbol{q}-\boldsymbol{\theta}) = \boldsymbol{0} \tag{1}$$

$$\boldsymbol{B}\ddot{\boldsymbol{\theta}} + \boldsymbol{D}_\theta\dot{\boldsymbol{\theta}} + \boldsymbol{K}(\boldsymbol{\theta}-\boldsymbol{q}) = \boldsymbol{\tau}, \tag{2}$$

where $\boldsymbol{M} > 0$ is the robot inertia matrix, the constant diagonal matrix $\boldsymbol{B} > 0$ contains the motor inertias, $\boldsymbol{c}$ is the vector of centrifugal and Coriolis terms, $\boldsymbol{g}$ is the gravity vector, $\boldsymbol{K} > 0$ is the diagonal matrix of joint stiffnesses, and $\boldsymbol{D}_q$ and $\boldsymbol{D}_\theta$ are positive semi-definite diagonal matrices of viscous friction coefficients. In terms of transmission deformation $\boldsymbol{\phi} = \boldsymbol{q} - \boldsymbol{\theta}$, the elastic potential $U_e = \frac{1}{2}\boldsymbol{\phi}^T\boldsymbol{K}\boldsymbol{\phi}$ associated to (1–2) leads to the *linear* elasticity torque vector $\boldsymbol{\tau}_e$ and *constant* device stiffness (diagonal) matrix $\boldsymbol{\sigma}$

$$\boldsymbol{\tau}_e = \left(\frac{\partial U_e}{\partial \boldsymbol{q}}\right)^T = \boldsymbol{K}\boldsymbol{\phi}, \qquad \boldsymbol{\sigma} = \frac{\partial \boldsymbol{\tau}_e}{\partial \boldsymbol{q}} = \boldsymbol{K}.$$

Our control goal is to define a (nonlinear) feedback law $\boldsymbol{\tau} = \boldsymbol{\tau}(\boldsymbol{q}, \boldsymbol{\theta}, \dot{\boldsymbol{q}}, \dot{\boldsymbol{\theta}}, \boldsymbol{\tau}_0)$ in (2) such that the behavior of the compensated system matches *in suitable coordinates* that of an identical model but without gravity, i.e.,

$$\boldsymbol{M}(\boldsymbol{q}_0)\ddot{\boldsymbol{q}}_0 + \boldsymbol{c}(\boldsymbol{q}_0, \dot{\boldsymbol{q}}_0) + \boldsymbol{D}_q\dot{\boldsymbol{q}}_0 + \boldsymbol{K}(\boldsymbol{q}_0 - \boldsymbol{\theta}_0) = \boldsymbol{0} \tag{3}$$

$$\boldsymbol{B}\ddot{\boldsymbol{\theta}}_0 + \boldsymbol{D}_\theta\dot{\boldsymbol{\theta}}_0 + \boldsymbol{K}(\boldsymbol{\theta}_0 - \boldsymbol{q}_0) = \boldsymbol{\tau}_0, \tag{4}$$

where the subscript 0 characterizes the variables of the robot *in the absence of gravity*.

It is well known [11] that system (1–2) is exactly linearizable by means of a static state feedback into decoupled chains of four integrators, with $\boldsymbol{q}$ and its first three time derivatives being the linearizing coordinates. Indeed, the same holds true also for system (3–4). Therefore, thanks to the feedback equivalence principle, by imposing the equality

$$\boldsymbol{q}(t) \equiv \boldsymbol{q}_0(t), \qquad \forall t \geq 0 \tag{5}$$

one should obtain the desired result without resorting to the complexity of a complete feedback linearization process. One challenge in the application of this simple idea is whether the solution can be found in closed form or not. Below, we show constructively that this is feasible for robots with elastic joints. The same conceptual steps will be followed in all considered instances of transmission flexibility, albeit in some cases the solution will require a numerical procedure.

Differentiating once eq. (1) w.r.t. time yields

$$\boldsymbol{M}(\boldsymbol{q})\boldsymbol{q}^{[3]} + (\dot{\boldsymbol{M}}(\boldsymbol{q}) + \boldsymbol{D}_q)\ddot{\boldsymbol{q}} + \dot{\boldsymbol{c}}(\boldsymbol{q}, \dot{\boldsymbol{q}}) + \dot{\boldsymbol{g}}(\boldsymbol{q}) + \boldsymbol{K}(\dot{\boldsymbol{q}} - \dot{\boldsymbol{\theta}}) = \boldsymbol{0},$$

with the notation $\boldsymbol{q}^{[i]} = d^i\boldsymbol{q}/dt^i$. Differentiating one more time, and substituting $\ddot{\boldsymbol{\theta}}$ from (2), we obtain

$$\begin{aligned}\boldsymbol{M}(\boldsymbol{q})\boldsymbol{q}^{[4]} + (2\dot{\boldsymbol{M}}(\boldsymbol{q}) + \boldsymbol{D}_q)\boldsymbol{q}^{[3]} + \ddot{\boldsymbol{M}}(\boldsymbol{q})\ddot{\boldsymbol{q}} + \ddot{\boldsymbol{c}}(\boldsymbol{q}, \dot{\boldsymbol{q}}) + \boldsymbol{K}\ddot{\boldsymbol{q}} \\ = \boldsymbol{K}\boldsymbol{B}^{-1}\left(\boldsymbol{\tau} - \boldsymbol{D}_\theta\dot{\boldsymbol{\theta}} - \boldsymbol{K}(\boldsymbol{\theta} - \boldsymbol{q})\right) - \ddot{\boldsymbol{g}}(\boldsymbol{q}).\end{aligned} \tag{6}$$

Noting that the left-hand side of (6) is a function of $\boldsymbol{q}$ and its first four derivatives only, we will write it compactly as $\boldsymbol{f}(\boldsymbol{q}, \ddot{\boldsymbol{q}}, \ddot{\boldsymbol{q}}, \boldsymbol{q}^{[3]}, \boldsymbol{q}^{[4]})$. Repeating the same computation for the no-gravity model (3–4) leads to

$$\boldsymbol{f}(\boldsymbol{q}_0, \ddot{\boldsymbol{q}}_0, \ddot{\boldsymbol{q}}_0, \boldsymbol{q}_0^{[3]}, \boldsymbol{q}_0^{[4]}) = \boldsymbol{K}\boldsymbol{B}^{-1}\left(\boldsymbol{\tau}_0 - \boldsymbol{D}_\theta\dot{\boldsymbol{\theta}}_0 - \boldsymbol{K}(\boldsymbol{\theta}_0 - \boldsymbol{q})\right). \tag{7}$$

By imposing (5), the left-hand sides of (6) and (7) will be equal, and thus

$$\begin{aligned}\boldsymbol{K}\boldsymbol{B}^{-1}\left(\boldsymbol{\tau} - \boldsymbol{D}_\theta\dot{\boldsymbol{\theta}} - \boldsymbol{K}(\boldsymbol{\theta} - \boldsymbol{q})\right) - \ddot{\boldsymbol{g}}(\boldsymbol{q}) \\ = \boldsymbol{K}\boldsymbol{B}^{-1}\left(\boldsymbol{\tau}_0 - \boldsymbol{D}_\theta\dot{\boldsymbol{\theta}}_0 - \boldsymbol{K}(\boldsymbol{\theta}_0 - \boldsymbol{q})\right).\end{aligned} \tag{8}$$

In order to eliminate the presence of the motor variables in (8), we use eqs. (1) and (3). By imposing again (5), one has

$$\begin{aligned}\boldsymbol{K}(\boldsymbol{\theta} - \boldsymbol{q}) &= \boldsymbol{M}(\boldsymbol{q})\ddot{\boldsymbol{q}} + \boldsymbol{c}(\boldsymbol{q}, \dot{\boldsymbol{q}}) + \boldsymbol{D}_q\dot{\boldsymbol{q}} + \boldsymbol{g}(\boldsymbol{q}) \\ \boldsymbol{K}(\boldsymbol{\theta}_0 - \boldsymbol{q}) &= \boldsymbol{M}(\boldsymbol{q})\ddot{\boldsymbol{q}} + \boldsymbol{c}(\boldsymbol{q}, \dot{\boldsymbol{q}}) + \boldsymbol{D}_q\dot{\boldsymbol{q}},\end{aligned} \tag{9}$$

or

$$\boldsymbol{\theta} = \boldsymbol{\theta}_0 + \boldsymbol{K}^{-1}\boldsymbol{g}(\boldsymbol{q}), \tag{10}$$

and then

$$\dot{\boldsymbol{\theta}} = \dot{\boldsymbol{\theta}}_0 + \boldsymbol{K}^{-1}\dot{\boldsymbol{g}}(\boldsymbol{q}). \tag{11}$$

Replacing eqs. (10–11) into (8) and simplifying, the solution to our problem is obtained by choosing the control law as

$$\boldsymbol{\tau} = \boldsymbol{\tau}_g + \boldsymbol{\tau}_0 \tag{12}$$

with

$$\boldsymbol{\tau}_g = \boldsymbol{g}(\boldsymbol{q}) + \boldsymbol{D}_\theta \boldsymbol{K}^{-1}\dot{\boldsymbol{g}}(\boldsymbol{q}) + \boldsymbol{B}\boldsymbol{K}^{-1}\ddot{\boldsymbol{g}}(\boldsymbol{q}), \tag{13}$$

where

$$\dot{\boldsymbol{g}}(\boldsymbol{q}) = \frac{\partial \boldsymbol{g}(\boldsymbol{q})}{\partial \boldsymbol{q}}\,\dot{\boldsymbol{q}}$$

$$\ddot{\boldsymbol{g}}(\boldsymbol{q}) = \frac{\partial \boldsymbol{g}(\boldsymbol{q})}{\partial \boldsymbol{q}}\boldsymbol{M}^{-1}(\boldsymbol{q})\big(\boldsymbol{K}(\boldsymbol{\theta}-\boldsymbol{q}) - \boldsymbol{c}(\boldsymbol{q},\dot{\boldsymbol{q}}) - \boldsymbol{g}(\boldsymbol{q}) - \boldsymbol{D}_q\dot{\boldsymbol{q}}\big) + \sum_{i=1}^{n}\frac{\partial^2 \boldsymbol{g}(\boldsymbol{q})}{\partial \boldsymbol{q}\,\partial q_i}\,\dot{\boldsymbol{q}}\,\dot{q}_i.$$

In addition, matched initial conditions should hold at time $t = 0$:

$$\begin{aligned} \boldsymbol{q}(0) &= \boldsymbol{q}_0(0) \qquad & \ddot{\boldsymbol{q}}(0) &= \ddot{\boldsymbol{q}}_0(0) \\ \dot{\boldsymbol{q}}(0) &= \dot{\boldsymbol{q}}_0(0) \qquad & \boldsymbol{q}^{[3]}(0) &= \boldsymbol{q}_0^{[3]}(0). \end{aligned} \tag{14}$$

Note that, thanks to the control law (12–13), the identities (14) will be enforced for all $t \geq 0$. The matching conditions (14) are not really a restriction. In fact, these conditions can be read in both directions: for a given initial state of the gravity-loaded system, we can always find an equivalent gravity-free system that has its initial state matched. This implies that the link coordinates of the two systems will evolve in the same way under the same command $\boldsymbol{\tau}_0$.

A notable feature is that the control solution can be computed in closed form. Moreover, in static conditions, i.e., with $\dot{\boldsymbol{q}} = \ddot{\boldsymbol{q}} = \boldsymbol{0}$, the gravity cancellation torque (13) becomes $\boldsymbol{\tau}_g = \boldsymbol{g}(\boldsymbol{q})$, as to be expected. Instead, in dynamic conditions $\boldsymbol{\tau}_g$ includes terms that are proportional to the inverse of the joint stiffness $\boldsymbol{K}$. Thus, the more rigid are the transmissions the less extra dynamic torque is needed for gravity cancellation. In the limit, for $\boldsymbol{K} \to \infty$, we recover the standard gravity cancellation torque of the rigid case also in dynamic conditions.

We remark that, despite of the need of inverting the robot inertia matrix $\boldsymbol{M}(\boldsymbol{q})$, the gravity cancellation torque (13) is much simpler than the expression of a feedback linearization control law, which involves in fact also the time derivatives of the model terms $\boldsymbol{M}(\boldsymbol{q})$ and $\boldsymbol{c}(\boldsymbol{q},\dot{\boldsymbol{q}})$ up to the second order.

Indeed, there are still differences in the state behavior between the gravity-free system (3–4) and system (1–2) under the gravity cancellation control law (12–13). While the two systems will evolve in an identical way when looking at the linearizing coordinates $\boldsymbol{q}(t) \equiv \boldsymbol{q}_0(t)$, the inverse mappings of this evolution in

terms of the respective motor variables will be different, as dictated by eqs. (10) and (11). This should not be surprising from a physical point of view: the gravity-loaded robot needs the presence of a deformation $\boldsymbol{q}-\boldsymbol{\theta} \neq \boldsymbol{q}-\boldsymbol{\theta}_0$ that dynamically balances the gravity on the link side. The control law (12–13) will only cancel the effects on the link (output) motion, which is what we actually need during robot interaction with the environment or a human.

The torque input $\boldsymbol{\tau}_0$ in (12) can be chosen according to the robot primary task, e.g., as in [2] for a torque-based robot reaction to detected collisions in pHRI. In this context, perfect gravity cancellation allows a link behavior during transients and at steady-state that is totally unaffected by gravity bias. Furthermore, for a regulation task to a desired link position $\boldsymbol{q}_d$, it can be shown that the *PD-type* control law

$$\boldsymbol{\tau}_0 = \boldsymbol{K}_P \left(\boldsymbol{q}_d - \boldsymbol{\theta} + \boldsymbol{K}^{-1}\boldsymbol{g}(\boldsymbol{q})\right) - \boldsymbol{K}_D \Big(\dot{\boldsymbol{\theta}} - \boldsymbol{K}^{-1}\frac{\partial \boldsymbol{g}(\boldsymbol{q})}{\partial \boldsymbol{q}}\,\dot{\boldsymbol{q}}\Big),$$

achieves global asymptotic stabilization for *any* $\boldsymbol{K}_P > 0$ and $\boldsymbol{K}_D > 0$, i.e., without the need of a strictly positive lower bound on $\boldsymbol{K}_P$. This result holds for any $\boldsymbol{K} > 0$, i.e., also for very soft joints. A formal proof of this result is presented in Sect. 3.

2.1 Simulation results

To illustrate the performance of the control law (12–13), it is sufficient to compare the behavior of a single link with an elastic joint in the absence of gravity and that under gravity but with dynamic gravity cancellation. In this case, the scalar link inertia M is constant and the gravity term is $g(q) = mdg_0 \sin q$, where m is the mass of the link, d is the distance of its center of mass from the joint, and g_0 is the gravity acceleration. The explicit expression of the dynamic gravity cancellation term τ_g in (13) is then

$$\begin{aligned}\tau_g = mdg_0 \Big\{ \big(1 - \tfrac{B}{K}\,\dot{q}^2\big) \sin q - \tfrac{B}{M}\tfrac{mdg_0}{K}\, \sin q \cos q \\ + \tfrac{MD_\theta - BD_q}{KM}\,\dot{q}\cos q + \tfrac{B}{M}(\theta - q)\cos q \Big\}.\end{aligned} \tag{15}$$

Using $M = 8.333$, $B = 50$ [N·mm·s^2/rad], $m = 0.1$ [kg], $d = 250$ [mm], $D_q = 0.1$, $D_\theta = 1$ [N·mm·s/rad], and $K = 100$ [N·mm/rad] as data, we simulated the two systems starting at rest from the downward equilibrium, and applying an open-loop torque $\tau_0 = \sin 0.1\pi t$ for $T = 10$ s. Figure 1 shows the obtained evolution of the link (a) and motor (b) angles in the absence or presence of gravity. For the latter case, we have considered also the use of a simpler link-based compensation $g(q)$ in place of the dynamic cancellation law τ_g given by (15). From Fig. 1(a), it can be seen that $q(t) = q_0(t)$ exactly in the case of dynamic cancellation, while an error is present when using $g(q)$. On the other hand, $\theta(t) \neq \theta_0(t)$ (both with dynamic cancellation and link-based compensation) despite the initial

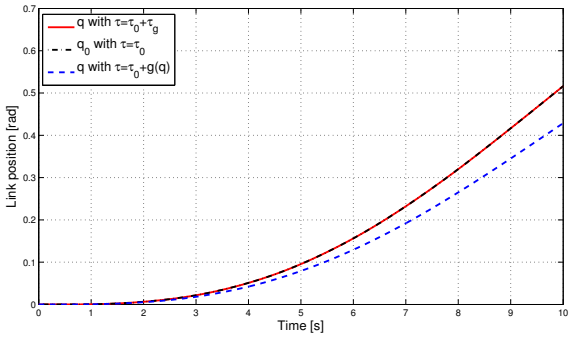

(a)

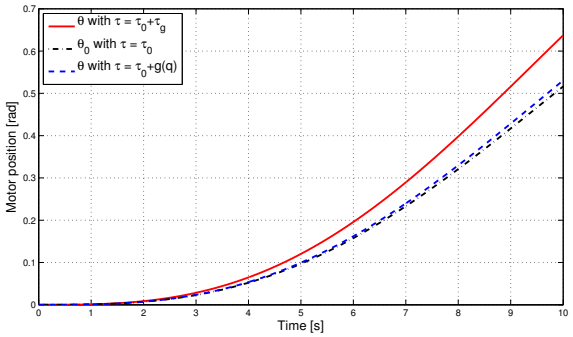

(b)

Figure 1: Comparison of link (a) and motor (b) position for a single elastic joint without gravity under τ_0 [dot-dashed, black], and with gravity under τ_0 and a link-based compensation $g(q)$ [dashed, blue] or under τ_0 and the dynamic cancellation law τ_g in (15) [continuous, red]

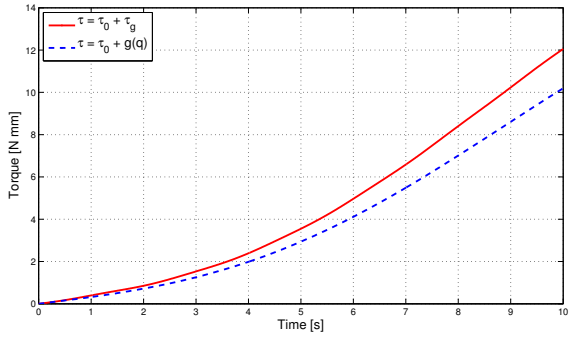

Figure 2: Total applied torques with $g(q)$ only [dashed, blue] and with τ_g in (15) [continuous, red] for the motion of Fig. 1

states of the systems with and without gravity were fully matched at $t = 0$, with no initial joint deformation (see Fig. 1(b)). The total torques (i.e., including τ_0) for the link-based gravity compensation and for its perfect cancellation are reported in Fig. 2, showing that the dynamic torque contribution is indeed non-negligible.

3 A New PD-type Regulator for Robots with Elastic Joints

Consider again the gravity-loaded system (1–2) in the absence of dissipative terms[1], i.e.,

$$\boldsymbol{M}(\boldsymbol{q})\ddot{\boldsymbol{q}} + \boldsymbol{S}(\boldsymbol{q},\dot{\boldsymbol{q}})\dot{\boldsymbol{q}} + \boldsymbol{g}(\boldsymbol{q}) + \boldsymbol{K}(\boldsymbol{q}-\boldsymbol{\theta}) = \boldsymbol{0} \tag{16}$$

$$\boldsymbol{B}\ddot{\boldsymbol{\theta}} + \boldsymbol{K}(\boldsymbol{\theta}-\boldsymbol{q}) = \boldsymbol{\tau}, \tag{17}$$

where any factorization $\boldsymbol{c}(\boldsymbol{q},\dot{\boldsymbol{q}}) = \boldsymbol{S}(\boldsymbol{q},\dot{\boldsymbol{q}})\dot{\boldsymbol{q}}$ can be used for the Coriolis/centrifugal vector. We address the problem of asymptotic stabilization of a desired (closed-loop) equilibrium state

$$\boldsymbol{q} = \boldsymbol{q}_d, \quad \boldsymbol{\theta} = \boldsymbol{\theta}_d := \boldsymbol{q}_d + \boldsymbol{K}^{-1}\boldsymbol{g}(\boldsymbol{q}_d), \quad \dot{\boldsymbol{q}} = \dot{\boldsymbol{\theta}} = \boldsymbol{0}. \tag{18}$$

The desired motor position $\boldsymbol{\theta}_d$ is obtained from the static analysis (i.e., setting $\dot{\boldsymbol{q}} = \ddot{\boldsymbol{q}} = \boldsymbol{0}$) of equation (16) at the desired link position $\boldsymbol{q}_d$.

Taking advantage of the dynamic gravity cancellation law, we present a new regulation controller realizing the task. The complete control law is defined as

$$\boldsymbol{\tau} = \boldsymbol{\tau}_g + \boldsymbol{\tau}_0, \tag{19}$$

where $\boldsymbol{\tau}_g$ is given by (13) (having set $\boldsymbol{D}_\theta = \boldsymbol{O}$)

$$\boldsymbol{\tau}_g = \boldsymbol{g}(\boldsymbol{q}) + \boldsymbol{B}\boldsymbol{K}^{-1}\ddot{\boldsymbol{g}}(\boldsymbol{q}), \tag{20}$$

and $\boldsymbol{\tau}_0$ is chosen as the *PD-type control law*

$$\boldsymbol{\tau}_0 = \boldsymbol{K}_P(\boldsymbol{q}_d - \boldsymbol{\theta} + \boldsymbol{K}^{-1}\boldsymbol{g}(\boldsymbol{q})) - \boldsymbol{K}_D(\dot{\boldsymbol{\theta}} - \boldsymbol{K}^{-1}\dot{\boldsymbol{g}}(\boldsymbol{q})). \tag{21}$$

The following result holds.

Theorem 1 *The desired state (18) for system (16–17) with control law (19–21) is the unique equilibrium state of the closed-loop system. Moreover, if*

$$\boldsymbol{K}_P > 0, \qquad \boldsymbol{K}_D > 0,$$

the desired state is globally asymptotically stable.

[1] Neglecting dissipative terms (e.g., viscous friction on the motor and link sides) is the worst situation from the point of view of stability of the robotic system. Their inclusion would make the analysis simpler.

Proof The proof is based on Lyapunov analysis and LaSalle theorem. First, we show that there is a unique equilibrium state for the closed-loop system, i.e., a unique equilibrium configuration $(\boldsymbol{q}_e, \boldsymbol{\theta}_e)$ with zero velocities $\dot{\boldsymbol{q}}$ and $\dot{\boldsymbol{\theta}}$. By setting $\ddot{\boldsymbol{q}} = \ddot{\boldsymbol{\theta}} = \mathbf{0}$ in the closed-loop equations given by (16–17) and (19–21), any equilibrium configuration should satisfy

$$\begin{aligned} \boldsymbol{g}(\boldsymbol{q}_e) + \boldsymbol{K}(\boldsymbol{q}_e - \boldsymbol{\theta}_e) &= \mathbf{0} \\ \boldsymbol{K}(\boldsymbol{q}_e - \boldsymbol{\theta}_e) + \boldsymbol{g}(\boldsymbol{q}_e) + \boldsymbol{K}_P(\boldsymbol{q}_d - \boldsymbol{\theta}_e + \boldsymbol{K}^{-1}\boldsymbol{g}(\boldsymbol{q}_e)) &= \mathbf{0}. \end{aligned}$$

Subtracting the two equations leads to

$$\boldsymbol{\theta}_e = \boldsymbol{q}_d + \boldsymbol{K}^{-1}\boldsymbol{g}(\boldsymbol{q}_e),$$

while the first equation yields

$$\boldsymbol{\theta}_e = \boldsymbol{q}_e + \boldsymbol{K}^{-1}\boldsymbol{g}(\boldsymbol{q}_e).$$

By comparison, it follows that the the unique equilibrium is

$$\boldsymbol{q}_e = \boldsymbol{q}_d, \qquad \boldsymbol{\theta}_e = \boldsymbol{q}_d + \boldsymbol{K}^{-1}\boldsymbol{g}(\boldsymbol{q}_d) = \boldsymbol{\theta}_d.$$

Let a Lyapunov candidate be defined by the following quadratic function:

$$\begin{aligned} V = \tfrac{1}{2}\Big(& \dot{\boldsymbol{q}}^T\boldsymbol{M}(\boldsymbol{q})\dot{\boldsymbol{q}} + \Big(\dot{\boldsymbol{\theta}} - \boldsymbol{K}^{-1}\dot{\boldsymbol{g}}(\boldsymbol{q})\Big)^T\boldsymbol{B}\Big(\dot{\boldsymbol{\theta}} - \boldsymbol{K}^{-1}\dot{\boldsymbol{g}}(\boldsymbol{q})\Big) \\ & + \big(\boldsymbol{q} - \boldsymbol{\theta} + \boldsymbol{K}^{-1}\boldsymbol{g}(\boldsymbol{q})\big)^T\boldsymbol{K}\big(\boldsymbol{q} - \boldsymbol{\theta} + \boldsymbol{K}^{-1}\boldsymbol{g}(\boldsymbol{q})\big) \\ & + \big(\boldsymbol{q}_d - \boldsymbol{\theta} + \boldsymbol{K}^{-1}\boldsymbol{g}(\boldsymbol{q})\big)^T\boldsymbol{K}_P\big(\boldsymbol{q}_d - \boldsymbol{\theta} + \boldsymbol{K}^{-1}\boldsymbol{g}(\boldsymbol{q})\big)\Big). \end{aligned}$$

As the sum of positive definite quadratic terms, V is positive definite. Moreover, $V = 0$ if and only if

$$\dot{\boldsymbol{q}} = \mathbf{0}, \quad \dot{\boldsymbol{\theta}} - \boldsymbol{K}^{-1}\frac{\partial \boldsymbol{g}(\boldsymbol{q})}{\partial \boldsymbol{q}}\dot{\boldsymbol{q}} = \mathbf{0} \quad \Rightarrow \quad \dot{\boldsymbol{\theta}} = \mathbf{0}$$

and

$$\left.\begin{aligned} \boldsymbol{q} - \boldsymbol{\theta} + \boldsymbol{K}^{-1}\boldsymbol{g}(\boldsymbol{q}) &= \mathbf{0} \\ \boldsymbol{q}_d - \boldsymbol{\theta} + \boldsymbol{K}^{-1}\boldsymbol{g}(\boldsymbol{q}) &= \mathbf{0} \end{aligned}\right\} \Rightarrow \left\{\begin{aligned} \boldsymbol{q} &= \boldsymbol{q}_d \\ \boldsymbol{\theta} &= \boldsymbol{q}_d + \boldsymbol{K}^{-1}\boldsymbol{g}(\boldsymbol{q}_d). \end{aligned}\right.$$

Therefore, the desired state is the unique minimum of V. Dropping for compactness dependencies, the time derivative of V is

$$\begin{aligned} \dot{V} = & \dot{\boldsymbol{q}}^T\boldsymbol{M}\ddot{\boldsymbol{q}} + \tfrac{1}{2}\dot{\boldsymbol{q}}^T\dot{\boldsymbol{M}}\dot{\boldsymbol{q}} + \Big(\dot{\boldsymbol{\theta}} - \boldsymbol{K}^{-1}\dot{\boldsymbol{g}}\Big)^T\boldsymbol{B}\Big(\ddot{\boldsymbol{\theta}} - \boldsymbol{K}^{-1}\ddot{\boldsymbol{g}}\Big) \\ & + \big(\boldsymbol{q} - \boldsymbol{\theta} + \boldsymbol{K}^{-1}\boldsymbol{g}\big)^T\boldsymbol{K}\left(\dot{\boldsymbol{q}} - \dot{\boldsymbol{\theta}} + \boldsymbol{K}^{-1}\dot{\boldsymbol{g}}\right) \\ & - \big(\boldsymbol{q}_d - \boldsymbol{\theta} + \boldsymbol{K}^{-1}\boldsymbol{g}\big)^T\boldsymbol{K}_P\left(\dot{\boldsymbol{\theta}} - \boldsymbol{K}^{-1}\dot{\boldsymbol{g}}\right). \end{aligned}$$

The closed-loop equations (16–17) with (19–21) can be conveniently rewritten in the form

$$\boldsymbol{M}\ddot{\boldsymbol{q}} = \boldsymbol{K}(\boldsymbol{\theta} - \boldsymbol{q}) - \boldsymbol{S}\dot{\boldsymbol{q}} - \boldsymbol{g}$$
$$\boldsymbol{B}\left(\ddot{\boldsymbol{\theta}} - \boldsymbol{K}^{-1}\ddot{\boldsymbol{g}}\right) = \boldsymbol{K}(\boldsymbol{q} - \boldsymbol{\theta}) + \boldsymbol{g} + \boldsymbol{K}_P\left(\boldsymbol{q}_d - \boldsymbol{\theta} + \boldsymbol{K}^{-1}\boldsymbol{g}\right) - \boldsymbol{K}_D\left(\dot{\boldsymbol{\theta}} - \boldsymbol{K}^{-1}\dot{\boldsymbol{g}}\right).$$

Substituting these into the expression of $\dot{V}$ and simplifying terms yields

$$\begin{aligned}
\dot{V} = {} & \dot{\boldsymbol{q}}^T\left(\boldsymbol{K}(\boldsymbol{\theta} - \boldsymbol{q}) + \tfrac{1}{2}\left(\dot{\boldsymbol{M}} - 2\boldsymbol{S}\right)\dot{\boldsymbol{q}} - \boldsymbol{g}\right) \\
& + \left(\dot{\boldsymbol{\theta}} - \boldsymbol{K}^{-1}\dot{\boldsymbol{g}}\right)^T\left(\boldsymbol{K}(\boldsymbol{q} - \boldsymbol{\theta}) + \boldsymbol{g}\right. \\
& \qquad \left. + \boldsymbol{K}_P\left(\boldsymbol{q}_d - \boldsymbol{\theta} + \boldsymbol{K}^{-1}\boldsymbol{g}\right) - \boldsymbol{K}_D\left(\dot{\boldsymbol{\theta}} - \boldsymbol{K}^{-1}\dot{\boldsymbol{g}}\right)\right) \\
& + \left(\boldsymbol{K}(\boldsymbol{q} - \boldsymbol{\theta}) + \boldsymbol{g}\right)^T\left(\dot{\boldsymbol{q}} - \dot{\boldsymbol{\theta}} + \boldsymbol{K}^{-1}\dot{\boldsymbol{g}}\right) \\
& - \left(\boldsymbol{q}_d - \boldsymbol{\theta} + \boldsymbol{K}^{-1}\boldsymbol{g}\right)^T\boldsymbol{K}_P\left(\dot{\boldsymbol{\theta}} - \boldsymbol{K}^{-1}\dot{\boldsymbol{g}}\right) \\
= {} & -\left(\dot{\boldsymbol{\theta}} - \boldsymbol{K}^{-1}\dot{\boldsymbol{g}}\right)^T\boldsymbol{K}_D\left(\dot{\boldsymbol{\theta}} - \boldsymbol{K}^{-1}\dot{\boldsymbol{g}}\right) \leq 0,
\end{aligned}$$

where the general relation $\dot{\boldsymbol{q}}^T\left(\dot{\boldsymbol{M}} - 2\boldsymbol{S}\right)\dot{\boldsymbol{q}} = \boldsymbol{0}$ has been used. Thus, it is

$$\dot{V} = 0 \quad \Leftrightarrow \quad \dot{\boldsymbol{g}}(\boldsymbol{q}) - \boldsymbol{K}\dot{\boldsymbol{\theta}} = \boldsymbol{0}.$$

We proceed by using LaSalle arguments. The desired state satisfies indeed $\dot{V} = 0$, and thus $V(t) \equiv 0$. We should verify whether there are other system trajectories that are invariant with respect to the set of states where $\dot{V} = 0$. When $\dot{V} = 0$, note first that

$$\frac{d}{dt}\left(\boldsymbol{g}(\boldsymbol{q}) - \boldsymbol{K}\boldsymbol{\theta}\right) = \boldsymbol{0} \quad \Rightarrow \quad \boldsymbol{g}(\boldsymbol{q}) - \boldsymbol{K}\boldsymbol{\theta} = \boldsymbol{k}_1,$$

where $\boldsymbol{k}_1$ is a constant vector. Moreover, the model equation (17) with $\boldsymbol{\tau}$ as in (19–21) becomes

$$\boldsymbol{B}\,\ddot{\boldsymbol{\theta}} + \boldsymbol{K}(\boldsymbol{\theta} - \boldsymbol{q}) = \boldsymbol{g}(\boldsymbol{q}) + \boldsymbol{B}\boldsymbol{K}^{-1}\ddot{\boldsymbol{g}}(\boldsymbol{q}) + \boldsymbol{K}_P(\boldsymbol{q}_d - \boldsymbol{\theta} + \boldsymbol{K}^{-1}\boldsymbol{g}(\boldsymbol{q})),$$

or, by simple manipulation,

$$\boldsymbol{B}\boldsymbol{K}^{-1}\frac{d}{dt}\left(\boldsymbol{K}\dot{\boldsymbol{\theta}} - \dot{\boldsymbol{g}}(\boldsymbol{q})\right) = \left(\boldsymbol{I} + \boldsymbol{K}_P\boldsymbol{K}^{-1}\right)\left[\boldsymbol{g}(\boldsymbol{q}) - \boldsymbol{K}\boldsymbol{\theta}\right] + \boldsymbol{K}\boldsymbol{q} + \boldsymbol{K}_P\boldsymbol{q}_d.$$

For a closed-loop system trajectory remaining in the set of states such that $\dot{V} = 0$, the left-hand side of this equation must be zero. Since the term in square brackets on the right-hand side is constant, it follows that

$$\boldsymbol{K}\boldsymbol{q} + \boldsymbol{K}_P\boldsymbol{q}_d = \boldsymbol{k}_2,$$

and hence $\boldsymbol{q}$ is constant by itself. As a consequence, $\boldsymbol{\theta}$ is also a constant, and thus $\dot{\boldsymbol{q}} = \dot{\boldsymbol{\theta}} = \boldsymbol{0}$. Therefore, the only invariant trajectory of the closed-loop system

that is compatible with $\dot{V} = 0$ is an equilibrium state. Since $\boldsymbol{q} = \boldsymbol{q}_d$, $\boldsymbol{\theta} = \boldsymbol{\theta}_d$, with $\dot{\boldsymbol{q}} = \dot{\boldsymbol{\theta}} = \mathbf{0}$, is the unique equilibrium, then the desired state is globally asymptotically stable thanks to LaSalle theorem. This completes the proof[2]. ∎

A series of remarks are in order:

- The expression of the control law (21) is logically derived from a pure PD scheme on the motor variables $\boldsymbol{\theta}_0$ and $\dot{\boldsymbol{\theta}}_0$ of the gravity-free system,

$$\begin{aligned}\boldsymbol{\tau}_0 &= \boldsymbol{K}_P(\boldsymbol{\theta}_{d0} - \boldsymbol{\theta}_0) - \boldsymbol{K}_D\dot{\boldsymbol{\theta}}_0 \\ &= \boldsymbol{K}_P(\boldsymbol{q}_d - \boldsymbol{\theta} + \boldsymbol{K}^{-1}\boldsymbol{g}(\boldsymbol{q})) - \boldsymbol{K}_D(\dot{\boldsymbol{\theta}} - \boldsymbol{K}^{-1}\dot{\boldsymbol{g}}(\boldsymbol{q})),\end{aligned}$$

  using the relations (10–11) between motor variables of the gravity-free system and of the gravity-loaded system under the action of dynamic gravity cancellation, and noting that the motor reference for the PD is $\boldsymbol{\theta}_{d0} = \boldsymbol{q}_d$ since gravitational effects are canceled by $\boldsymbol{\tau}_g$. Another way of interpreting terms in the control law (19–21) is to note that the motor reference $\boldsymbol{\theta}_d = \boldsymbol{q}_d + \boldsymbol{K}^{-1}\boldsymbol{g}(\boldsymbol{q}_d)$ in the PD law with *constant* gravity compensation of [7] is replaced by its *on-line* version $\boldsymbol{q}_d + \boldsymbol{K}^{-1}\boldsymbol{g}(\boldsymbol{q})$.

- The PD term in the control law, i.e., eq. (21), needs feedback from the full state of the robot, just as the term $\boldsymbol{\tau}_g$. This is the same requisite of exact linearization laws by static state feedback. Conversely, energy-based Lyapunov designs for elastic joint robots use only motor feedback. The proposed controller realizes thus a compromise, eliminating the gravity-dependent dynamic terms by means of a full state feedback but avoiding the need of complete cancellation of the dynamics of the elastic joint robot.

- Using gravity cancellation, there is no need of a positive lower bound on the joint stiffness $\boldsymbol{K}$, as opposed to the previous literature [7, 8, 9]. While in practice joint stiffness always dominates the gradient of gravity torques in industrial robots with elastic joints (e.g., using harmonic drives), this relaxation can be of interest for actuation systems with variable stiffness (see Sect. 5), where very low values of stiffness may be desirable to limit injuries due to accidental collisions between robot and humans.

- Looking at the proof of Theorem 1, it is easy to see that the desired state would still be the unique equilibrium for the closed-loop system when reducing the gravity-term in the controller to $\boldsymbol{\tau}_g = \boldsymbol{g}(\boldsymbol{q})$. However, a Lyapunov-based proof of global asymptotic stability with such a term added to a PD controller is not available.

[2]The introduced constants are $\boldsymbol{k}_1 = -\boldsymbol{K}\boldsymbol{q}_d$, $\boldsymbol{k}_2 = (\boldsymbol{K} + \boldsymbol{K}_P)\boldsymbol{q}_d$.

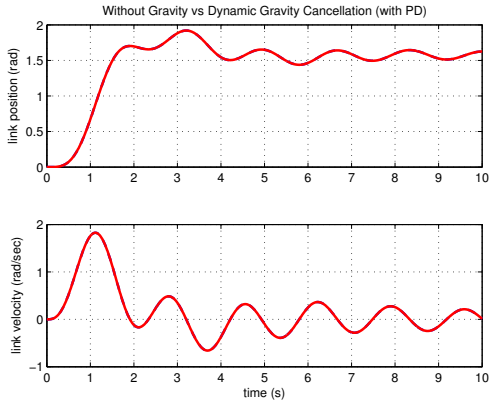

(a)

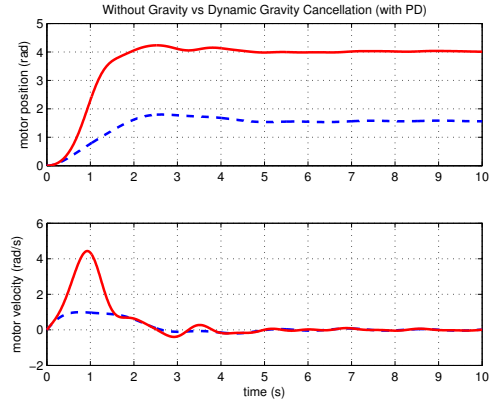

(b)

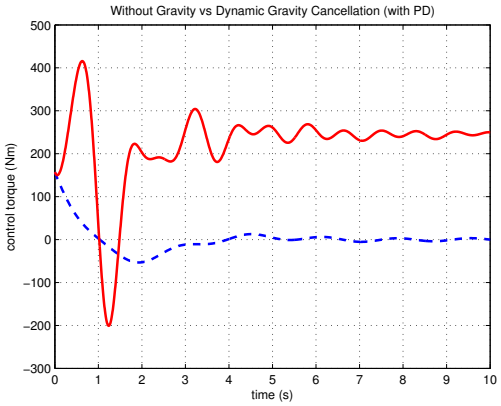

(c)

Figure 3: Comparison of link variables (a), motor variables (b), and control torques (c) for a single link with elastic joint without gravity under PD control on the motor side [dashed, blue], and with gravity under the PD-type control law with dynamic cancellation (19–21) [continuous, red]; the joint stiffness is $K = 100$

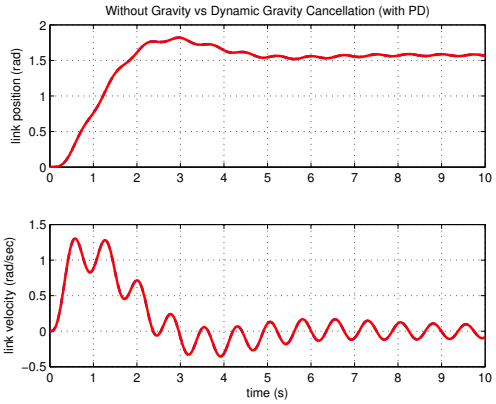

(a)

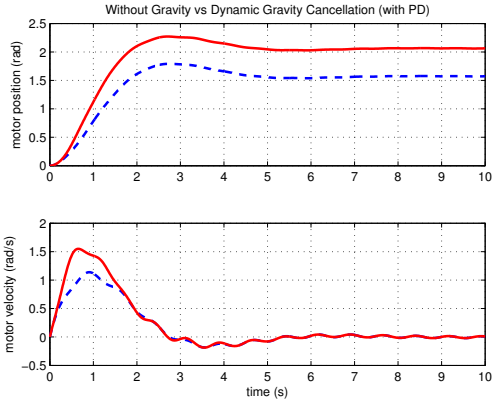

(b)

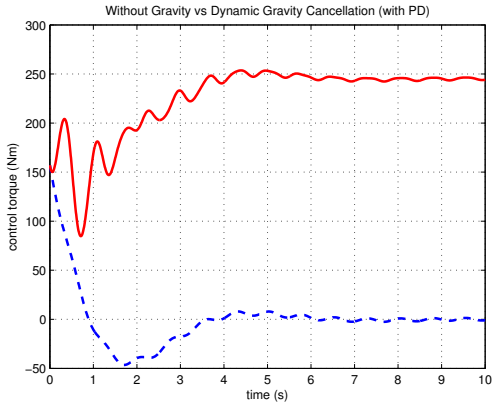

(c)

Figure 4: Comparison of link variables (a), motor variables (b), and control torques (c) for a single link with elastic joint without gravity under PD control on the motor side [dashed, blue], and with gravity under the PD-type control law with dynamic cancellation (19–21) [continuous, red]; the joint stiffness is $K = 500$

3.1 Simulation results

We present some simulation results that show the typical behavior obtained under the action of the PD-type control law (21) with the gravity cancellation (20). A single link with elastic joint is considered, using the same numerical data of Sect. 2.1. The link is commanded to move from the downward equilibrium $q = 0$ to $q_d = \pi/2$. The PD (scalar) gains were chosen as $k_P = 100$ and $k_D = 80$. These values were conveniently tuned in the absence of gravity. Figure 3 shows the comparative evolution of the relevant variables in the two situations of no gravity and presence of gravity with gravity cancellation. The link motion in Fig. 3(a) is exactly the same, as expected. The motor position has a different evolution in the two cases (Fig. 3(b)), due to the need to charge the elastic joint for dynamically balancing gravity on the link. The total applied motor torque is also different (Fig. 3(c)): in fact, it should vanish at steady state when gravity is absent, whereas it should at least provide the static gravity torque at final destination in the other case. On the other hand, the PD component of the new control law is exactly the same as the PD action in the absence of gravity (plots not shown).

The new control law is able to regulate the link to the desired position even if the joint stiffness is here very small, in particular lower than the maximum gradient of the gravity term ($K = 100 < 245.25 = mdg_0$). Note that the small oscillations experienced by the link while approaching the goal are due to the poor transient performance achievable by motor PD feedback in the absence of gravity, and not to the nature of the dynamic gravity cancellation law: the only role of τ_g is to allow the exact reproduction of the link behavior in the absence of gravity, no matter how good or bad this is[3]. The very low value of joint stiffness is partly responsible for this behavior. In fact, Figure 4 shows the results under the same PD gains when increasing the joint stiffness to $K = 500$. The improvement in the transient behavior is quite apparent.

4 Joints with Nonlinear Flexibility

In this section, we extend the analysis of Sect. 2 to the case of transmissions with nonlinear flexibility [23]. For the sake of simplicity, only a single dof will be considered, but the generalization to multi-dof systems is straightforward. Using the same notation of Sec. 2, we assume that a potential energy $U_e(\phi) \geq 0$ is associated to the deformation $\phi = q - \theta$, so that the flexibility torque $\tau_e = \partial U_e/\partial q = \tau_e(\phi)$ is a nonlinear function of ϕ and the stiffness $\sigma = \partial \tau_e/\partial q = \sigma(\phi)$ will be nonconstant.

The dynamic model of a single link moving *under gravity* and driven through

[3]We have also used the `Simulink Design Optimization` tool of Matlab for tuning the PD gains in the absence of gravity, leading to the choice $k_P = 41.3291$, $k_D = 87.1717$. While the control peaking in the first couple of seconds is eliminated, the transient response is somewhat slower and the link oscillations are practically left the same.

such a flexible transmission is then

$$M\ddot{q} + D_q\dot{q} + g(q) + \tau_e(\phi) = 0 \tag{22}$$

$$B\ddot{\theta} + D_\theta\dot{\theta} - \tau_e(\phi) = \tau. \tag{23}$$

We wish to define a feedback law $\tau = \tau(q, \theta, \dot{q}, \dot{\theta}, \tau_0)$ in (23) so as to match the behavior of some output variable of the model *without gravity*

$$M\ddot{q}_0 + D_q\dot{q}_0 + \tau_e(\phi_0) = 0 \tag{24}$$

$$B\ddot{\theta}_0 + D_\theta\dot{\theta}_0 - \tau_e(\phi_0) = \tau_0. \tag{25}$$

It is easy to verify that both nonlinear systems (22–23) and (24–25) are exactly linearizable by means of a static state feedback into a chain of four integrators, with q and its first three time derivatives as linearizing coordinates. Therefore, the two systems are feedback equivalent and the solution to our problem is obtained by imposing $q(t) = q_0(t)$ for all $t \geq 0$. In particular, from $q^{[4]} = q_0^{[4]}$ we get

$$\begin{aligned}\tau = {} & g(q) + \frac{D_\theta}{\sigma(\phi)}\,\dot{g}(q) + \frac{B}{\sigma(\phi)}\,\ddot{g}(q) \\ & + \frac{\sigma(\phi) - \sigma(\phi_0)}{\sigma(\phi)}\left((B+M)\ddot{q} + (D_q + D_\theta)\dot{q}\right) \\ & + \frac{B}{\sigma(\phi)}\left(\frac{\partial\sigma(\phi)}{\partial\phi}\,\dot{\phi}^2 - \frac{\partial\sigma(\phi_0)}{\partial\phi_0}\,\dot{\phi}_0^2\right) + \frac{\sigma(\phi_0)}{\sigma(\phi)}\,\tau_0 \\ = {} & \tau_g + \alpha_g\tau_0,\end{aligned} \tag{26}$$

where $\ddot{q}$ (to be used also in $\ddot{g}(q)$) is computed from (22) as

$$\ddot{q} = -\frac{1}{M}\left(D_q\dot{q} + g(q) + \tau_e(\phi)\right).$$

In addition, the initial matching requires

$$\begin{aligned} q(0) &= q_0(0) & \ddot{q}(0) &= \ddot{q}_0(0) \\ \dot{q}(0) &= \dot{q}_0(0) & q^{[3]}(0) &= q_0^{[3]}(0). \end{aligned} \tag{27}$$

Note that (26) collapses into (12–13) for a transmission with constant stiffness $\sigma = K$. However, differently from the case of linear elasticity, the control law (26) contains terms that require the knowledge of the deformation $\phi_0 = q - \theta_0$, and of its rate $\dot{\phi}_0$, pertaining to the model without gravity. Also, the torque τ_0 applied in the gravity-free case needs now to be scaled by the factor $\alpha_g = \sigma(\phi_0)/\sigma(\phi)$.

The value ϕ_0 is computed by solving the nonlinear equation $\tau_e(\phi_0) = -M\ddot{q} - D_q\dot{q}$, which is obtained from (24) by taking into account the first three identities in (27). Using (22), the right-hand side can be written as a function of the *state* (actually, of the configuration variables only) of the gravity-loaded system as

$$\tau_e(\phi_0) = g(q) + \tau_e(\phi) = a(q, \theta). \tag{28}$$

Equation (28) needs to be solved for ϕ_0 at each time $t \geq 0$ as a function of the current system state. As a representative example, consider a flexible joint transmission with associated potential given by $U_e = \frac{1}{2}K\phi^2 + \frac{1}{4}K_c\phi^4$, with $K > 0$ and $K_c > 0$. The flexibility torque is a cubic function of ϕ and the stiffness has a *quadratic* dependence:

$$\tau_e(\phi) = K\phi + K_c\phi^3, \qquad \sigma(\phi) = K + 3K_c\phi^2. \tag{29}$$

At a given (q, θ), equation (28) results in the cubic equation $K_c\phi_0^3 + K\phi_0 - a(q,\theta) = 0$, which has always two complex roots and one real (positive or negative) root, thanks to the positivity of K and K_c. The real root is given by

$$\phi_0 = \sqrt[3]{\frac{1}{2}\frac{a(q,\theta)}{K_c} + b(q,\theta)} + \sqrt[3]{\frac{1}{2}\frac{a(q,\theta)}{K_c} - b(q,\theta)},$$

where $b(q,\theta) = \sqrt{\frac{1}{27}\left(\frac{K}{K_c}\right)^3 + \frac{1}{4}\left(\frac{a(q,\theta)}{K_c}\right)^2} > 0$. For more general stiffness profiles, a solution to (28) should be searched numerically.

Once ϕ_0 has been found, the value of $\dot{\phi}_0$ that appears in the control law (26) is obtained by time differentiation of (28) (or, equivalently, from the fourth identity in (27)) as

$$\dot{\phi}_0 = \frac{1}{\sigma(\phi_0)}\left(\sigma(\phi)\dot{\phi} + \frac{\partial g(q)}{\partial q}\,\dot{q}\right). \tag{30}$$

As a result, the gravity cancellation control law (26) can be computed in closed form from full state measurements in the case of cubic stiffness (and for other simple nonlinear dependencies). Note that for multi-dof robots with nonlinear flexible joints one needs to solve n similar equations of the form (28), whereas (30) is replicated component-wise.

4.1 Simulation results

We simulated a joint with cubic flexibility torque $\tau_e(\phi)$ having $K = 100$ [N·mm/rad] and $K_c = 500$ [N·mm/rad]. With these data, the joint stiffness $\sigma(\phi)$ increases by about 45% w.r.t. its value at $\phi = 0$ when the joint deformation is $|\phi| = 0.18$ [rad]. All other model parameters, the initial conditions, and the open-loop input torque are the same as in Sect. 2.1. Figure 5 shows the evolution of the link (a) and motor (b) angles obtained in the absence or in the presence of gravity under the dynamic gravity cancellation law (26).

5 Variable Stiffness Joints with Antagonistic Actuation

Progressing in the generalization of our dynamic gravity cancellation approach, we consider in this section the case of joints with (actuated) variable stiffness. Use of variable nonlinear stiffness actuation is highly recommended for safe pHRI, with

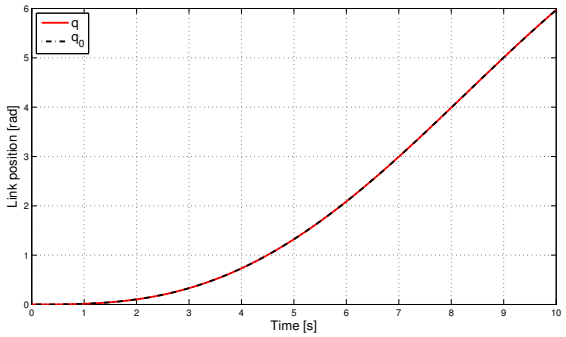

(a)

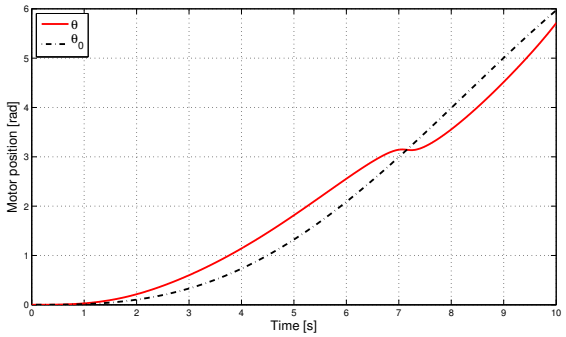

(b)

Figure 5: Comparison of link (a) and motor (b) position for a single nonlinear flexible joint without gravity under τ_0 [dot-dashed, black], and with gravity under the dynamic cancellation law (26) [continuous, red]

the antagonistic arrangement of two motors for each joint as the most common realization [13, 15, 16].

For the sake of notational simplicity, consider a single link under gravity driven by an antagonistic VSA system. The dynamic model is expressed in terms of three generalized coordinates, q for the link position, and θ_1 and θ_2 for the position of the two motors. Let $\phi_i = q - \theta_i$, $i = 1, 2$, be the deformations of the transmissions at the two sides of the joint. We have

$$M\ddot{q} + D_q\dot{q} + g(q) + \tau_e(\phi_1) + \tau_e(\phi_2) = 0 \tag{31}$$

$$B\ddot{\theta}_1 + D_\theta\dot{\theta}_1 - \tau_e(\phi_1) = \tau_1 \tag{32}$$

$$B\ddot{\theta}_2 + D_\theta\dot{\theta}_2 - \tau_e(\phi_2) = \tau_2, \tag{33}$$

where τ_1 and τ_2 are the torques supplied by the two motors. Without loss of generality, we have assumed in (31–33) a full symmetry for the two actuation/transmission systems. Accordingly, the total stiffness σ_t of the device is given by the separable

function

$$\sigma_t(\phi_1, \phi_2) = \frac{\partial(\tau_e(\phi_1) + \tau_e(\phi_2))}{\partial q} = \sigma(\phi_1) + \sigma(\phi_2). \tag{34}$$

As before, the target behavior is specified by a dynamic system of the same form (31–33), but with $g(q) \equiv 0$ and all its variables labeled by a 0 subscript.

Since the system has two inputs, according to the feedback equivalence principle, we should determine *two* independent system output functions that play the role of linearizing coordinates in a feedback linearization scheme. Based on the results in [21], these two outputs are the link position q and the total stiffness σ_t. In fact, differentiating once (31) w.r.t. time gives

$$M q^{[3]} + D_q \ddot{q} + \dot{g}(q) + \sigma(\phi_1)\dot{\phi}_1 + \sigma(\phi_2)\dot{\phi}_2 = 0. \tag{35}$$

DIfferentiating once more, using (32–33), and rearraging terms, we obtain

$$\begin{aligned} M q^{[4]} + D_q q^{[3]} + \ddot{g}(q) + \frac{\partial \sigma(\phi_1)}{\partial \phi_1}\dot{\phi}_1^2 + \frac{\partial \sigma(\phi_2)}{\partial \phi_2}\dot{\phi}_2^2 + \sigma_t \ddot{q} & \\ = \sigma(\phi_1)\ddot{\theta}_1 + \sigma(\phi_2)\ddot{\theta}_2 & \\ = \frac{1}{B}\begin{pmatrix} \sigma(\phi_1) & \sigma(\phi_2) \end{pmatrix} \begin{pmatrix} \tau_1 + \tau_e(\phi_1) - D_\theta \dot{\theta}_1 \\ \tau_2 + \tau_e(\phi_2) - D_\theta \dot{\theta}_2 \end{pmatrix}. & \end{aligned} \tag{36}$$

Similarly, by differentiating (34) w.r.t. time, we have

$$\dot{\sigma}_t = \frac{\partial \sigma(\phi_1)}{\partial \phi_1}\dot{\phi}_1 + \frac{\partial \sigma(\phi_2)}{\partial \phi_2}\dot{\phi}_2 \tag{37}$$

and, by rearraging terms and using again (32–33),

$$\begin{aligned} \ddot{\sigma}_t &= \frac{\partial^2 \sigma(\phi_1)}{\partial \phi_1^2}\dot{\phi}_1^2 + \frac{\partial^2 \sigma(\phi_2)}{\partial \phi_2^2}\dot{\phi}_2^2 + \left(\frac{\partial \sigma(\phi_1)}{\partial \phi_1} + \frac{\partial \sigma(\phi_2)}{\partial \phi_2}\right)\ddot{q} \\ &= \frac{\partial \sigma(\phi_1)}{\partial \phi_1}\ddot{\theta}_1 + \frac{\partial \sigma(\phi_2)}{\partial \phi_2}\ddot{\theta}_2 \\ &= \frac{1}{B}\begin{pmatrix} \dfrac{\partial \sigma(\phi_1)}{\partial \phi_1} & \dfrac{\partial \sigma(\phi_2)}{\partial \phi_2} \end{pmatrix} \begin{pmatrix} \tau_1 + \tau_e(\phi_1) - D_\theta \dot{\theta}_1 \\ \tau_2 + \tau_e(\phi_2) - D_\theta \dot{\theta}_2 \end{pmatrix}. \end{aligned} \tag{38}$$

It can be shown that the decoupling matrix associated to the output vector (q, σ_t) is proportional to the matrix

$$\boldsymbol{\mathcal{A}}(\phi_1, \phi_2) = \begin{pmatrix} \sigma(\phi_1) & \sigma(\phi_2) \\ \dfrac{\partial \sigma(\phi_1)}{\partial \phi_1} & \dfrac{\partial \sigma(\phi_2)}{\partial \phi_2} \end{pmatrix},$$

which is generically *nonsingular*, except when $\theta_1 = \theta_2$ (a condition that can always be avoided by suitably pre-charging the actuation system). Therefore, the

outputs q, together with its first three derivatives, and σ_t, with its first derivative, are linearizing coordinates for system (31–33).

Comparing the expressions (36) and (38) with those of the gravity-free case (with a 0 subscript), the solution to the problem of dynamic gravity cancellation is given by the control torques τ_1 and τ_2

$$\begin{aligned}\begin{pmatrix} \tau_1 \\ \tau_2 \end{pmatrix} = & \begin{pmatrix} D_\theta\,\dot\theta_1 - \tau_e(\phi_1) \\ D_\theta\,\dot\theta_2 - \tau_e(\phi_2) \end{pmatrix} + \boldsymbol{\mathcal{A}}^{-1}(\phi_1,\phi_2)\cdot \\ & \left\{ \boldsymbol{\mathcal{A}}(\phi_{10},\phi_{20}) \left(\begin{pmatrix} \tau_{10} \\ \tau_{20} \end{pmatrix} + \begin{pmatrix} \tau_e(\phi_{10}) - D_\theta\,\dot\theta_{10} \\ \tau_e(\phi_{20}) - D_\theta\,\dot\theta_{20} \end{pmatrix} \right) \right. \\ & \left. + B \begin{pmatrix} \ddot g(q) + \displaystyle\sum_{i=1}^{2} \left(\frac{\partial\sigma(\phi_i)}{\partial\phi_i}\,\dot\phi_i^2 - \frac{\partial\sigma(\phi_{i0})}{\partial\phi_{i0}}\,\dot\phi_{i0}^2 \right) \\ \displaystyle\sum_{i=1}^{2} \left(\frac{\partial\sigma(\phi_i)}{\partial\phi_i} - \frac{\partial\sigma(\phi_{i0})}{\partial\phi_{i0}} \right) \ddot q \\ \displaystyle\sum_{i=1}^{2} \left(\frac{\partial^2\sigma(\phi_i)}{\partial\phi_i^2}\,\dot\phi_i^2 - \frac{\partial^2\sigma(\phi_{i0})}{\partial\phi_{i0}^2}\,\dot\phi_{i0}^2 \right) \end{pmatrix} \right\}, \end{aligned} \tag{39}$$

where the link acceleration $\ddot q$ (to be used also in $\ddot g(q)$) is computed from (31) as

$$\ddot q = -\frac{1}{M}\left(D_q\dot q + g(q) + \tau_e(\phi_1) + \tau_e(\phi_2)\right).$$

In addition, an initial state matching given by

$$q(0) = q_0(0) \quad \dot q(0) = \dot q_0(0) \quad \ddot q(0) = \ddot q_0(0) \quad q^{[3]}(0) = q_0^{[3]}(0)$$

and

$$\begin{aligned} \sigma_t(0) = \sigma_t(\phi_1(0),\phi_2(0)) &= \sigma_t(\phi_{10}(0),\phi_{20}(0)) = \sigma_{t0}(0) \\ \dot\sigma_t(0) &= \dot\sigma_{t0}(0) \end{aligned}$$

should hold between the gravity-loaded and the gravity-free system. Note that the above identities will hold for all $t \geq 0$ thanks to the chosen control law.

The control law (39) physically replaces all terms that are affected by gravity (motor variables, flexible deformation torques, partial derivatives of the stiffness functions) with those of the gravity-free target system. For the considered single-dof VSA-based joint, the dynamic gravity cancellation law is very similar to a feedback linearization law from the point of view of complexity. However, these two controllers will differ consistently when considering multi-dof VSA robotic systems —in much the same way as for the case of single actuation of linear or nonlinear flexible joints.

Beside measurements of the state of the gravity-loaded system, in order to evaluate (39) we need also knowledge of the deformations ϕ_{i0}, $i = 1, 2$, and of their rates $\dot\phi_{i0}$, $i = 1, 2$, pertaining to the target system without gravity. Note

that from ϕ_{i0}, we directly obtain also $\theta_{i0} = q - \phi_{i0}$. Similarly to Sect. 4, the deformations ϕ_{10} and ϕ_{20} are determined by solving the coupled system of two nonlinear equations

$$\begin{aligned} \tau_e(\phi_{10}) + \tau_e(\phi_{20}) &= -M\ddot{q} - D_q\dot{q} = a_1(q, \theta_1, \theta_2) \\ \sigma(\phi_{10}) + \sigma(\phi_{20}) &= \sigma_t(q, \theta_1, \theta_2), \end{aligned} \tag{40}$$

where the right-hand sides of (40) are expressed in terms of current state measurements using (31) and (34). Due to the symmetry, if (ϕ_a, ϕ_b) is a solution of (40) then (ϕ_b, ϕ_a) is a solution as well.

In general, system (40) needs to be solved numerically. Some additional insight is provided in the case of *cubic* flexibility torques, see (29). We have then

$$K(\phi_{10} + \phi_{20}) + K_c(\phi_{10}^3 + \phi_{20}^3) = a_1(q, \theta_1, \theta_2) \tag{41}$$

$$2K + 3K_c(\phi_{10}^2 + \phi_{20}^2) = \sigma_t(q, \theta_1, \theta_2). \tag{42}$$

Since by definition

$$\frac{\sigma_t - 2K}{3K_c} := R^2 \geq 0,$$

the solutions to equation (42) can be parametrized by a scalar $\alpha \in [0, 2\pi)$ as $\phi_{10} = R\cos\alpha$ and $\phi_{20} = R\sin\alpha$. Replacing these in (41) yields the single trigonometric equation in α

$$(\cos\alpha + \sin\alpha) + \frac{\sigma_t - 2K}{3K}\left(\cos^3\alpha + \sin^3\alpha\right) = \frac{a_1}{KR}. \tag{43}$$

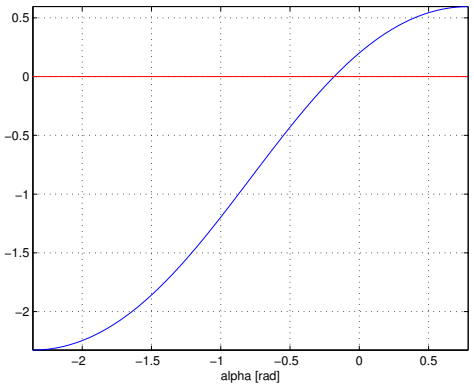

Figure 6: A typical functional form of eq. (43) and a possible solution

Figure 6 shows a plot of one of the two branches of the expression on the left-hand side of (43), obtained for $K = 100$, $K_c = 500$, and $\sigma_t = 220$. The horizontal line corresponds to the case $a_1 = 10$, and the associated root α provides the solution $\phi_{10} = 0.1136$ and $\phi_{20} = -0.0209$ [rad]. It can be seen that equation (43)

is sufficiently smooth, and thus easily solvable by a numerical root finder (e.g., the `fzero` routine of Matlab). Assume now that the device stiffness σ_t can be changed within the interval $(2K, 4K)$, i.e., from its minimum physical value to a 100% increase. It can be shown that a pair of α solutions to (43) always exist in this interval for σ_t, provided that $|a_1| < \sqrt{2}KR\,[1 + 0.5(\sigma_t - 2K)/(3K)]$.

It should be stressed that the existence of pairs of solutions is not a source of problems. In fact, system (40) will be solved at every (discretized) instant $t \geq 0$. Once a specific solution has been chosen at $t = 0$, the process is repeated on line and a local numerical search around the previous solution generates a single update.

FInally, having determined ϕ_{10} and ϕ_{20}, their rates are obtained by time differentiation of (40) as

$$\begin{aligned}\begin{pmatrix} \dot{\phi}_{10} \\ \dot{\phi}_{20} \end{pmatrix} &= \boldsymbol{\mathcal{A}}^{-1}(\phi_{10}, \phi_{20}) \begin{pmatrix} -Mq^{[3]} - D_q \ddot{q} \\ \dot{\sigma}_t \end{pmatrix} \\ &= \boldsymbol{\mathcal{A}}^{-1}(\phi_{10}, \phi_{20}) \begin{pmatrix} \sigma(\phi_1)\dot{\phi}_1 + \sigma(\phi_2)\dot{\phi}_2 + \frac{\partial g(q)}{\partial q}\,\dot{q} \\ \frac{\partial \sigma(\phi_1)}{\partial \phi_1}\,\dot{\phi}_1 + \frac{\partial \sigma(\phi_2)}{\partial \phi_2}\,\dot{\phi}_2 \end{pmatrix},\end{aligned}$$

where (35) and (37) have been used to express all quantities in terms of the original VSA system state only.

5.1 Simulation results

We have simulated the dynamic gravity cancellation law (39) for a symmetric antagonistic joint with cubic flexibility torques, using the numerical data of Sec. 4.1 duplicated as needed. In the present case, the input torques τ_{10} and τ_{20} have been chosen of the bang-bang type as in Fig. 7(c). Figure 7 shows the validity of the proposed scheme: both the link position (a) and the device stiffness (b) have identical evolutions in the absence of gravity and when gravity is present but dynamically canceled. Note that the stiffness variation during motion is as large as 2.5 [Nm/rad]. The total applied torques are shown in Fig. 8.

5.2 The VSA-II Variable Stiffness Joint

We report also a numerical result on gravity cancellation for the VSA-II experimental device developed at the University of Pisa [16] and sketched in Fig. 9. The VSA-II is based on a bi-directional antagonistic arrangement of two motors driving a single joint through a nonlinear flexible transmission system that uses pairs of 4-bar mechanisms (the so-called Grashof neutral linkage) with linear springs.

The VSA-II dynamic model takes the form (31–33), with

$$\tau_e(\phi_i) = 2K\,\beta(\phi_i)\,\frac{\partial \beta(\phi_i)}{\partial \phi_i}, \qquad i = 1, 2,$$

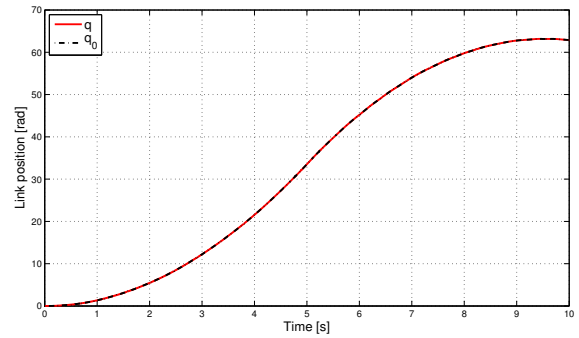

(a)

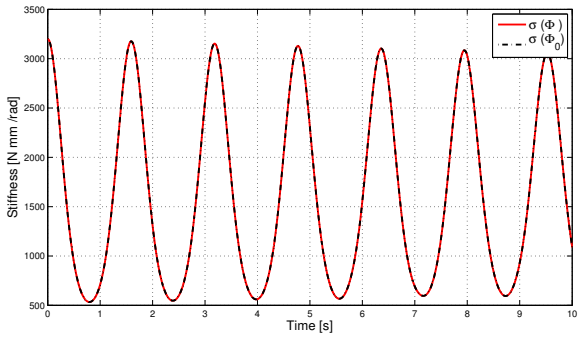

(b)

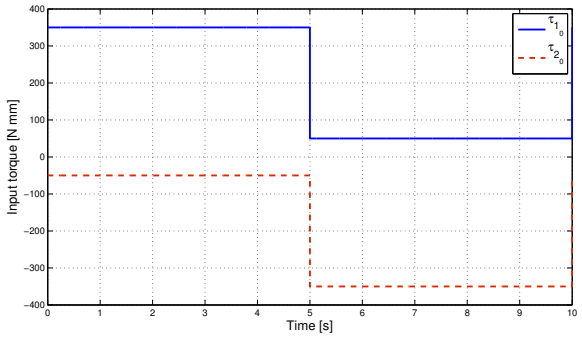

(c)

Figure 7: Comparison of link position (a) and device stiffness (b) for a variable stiffness antagonistic joint with cubic flexibility torques without gravity [dot-dashed, black], and with gravity under the dynamic cancellation law (39) [continuous, red] when the bang-bang torque inputs τ_{10} and τ_{10} (c) are applied

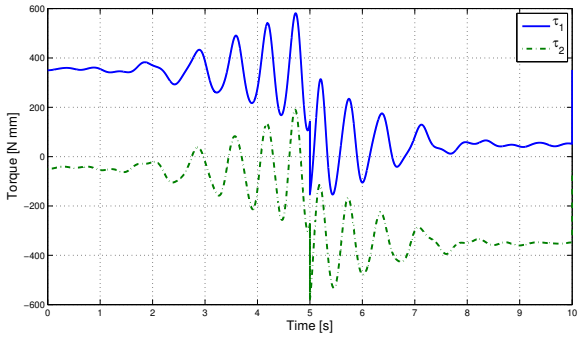

Figure 8: Total applied torques (39) for the link motion and device stiffness evolution of Fig. 7

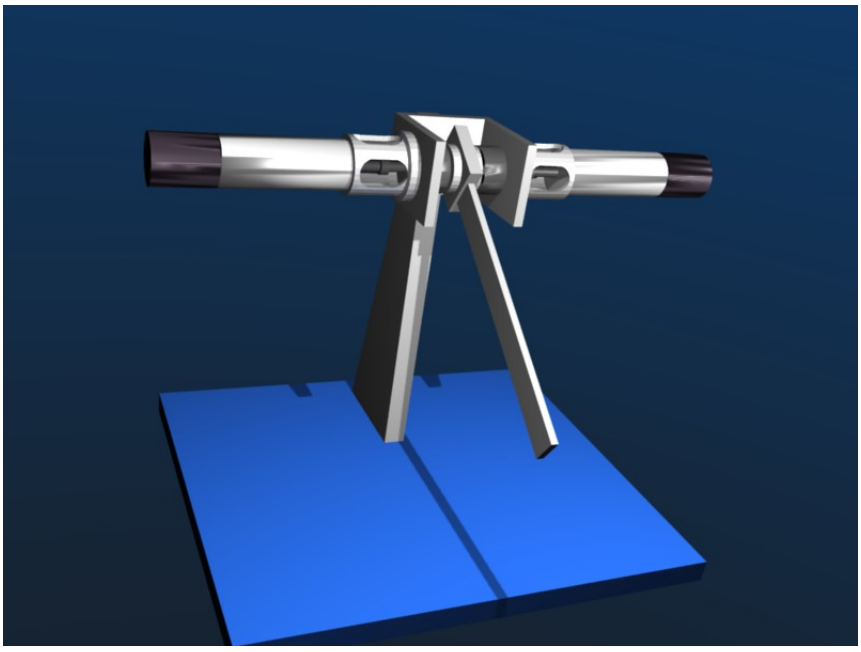

Figure 9: The VSA-II variable stiffness actuator moving a link under gravity

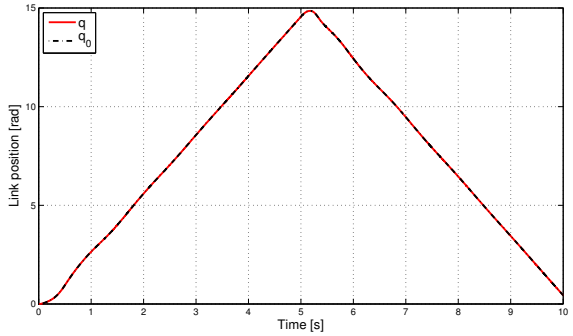

(a)

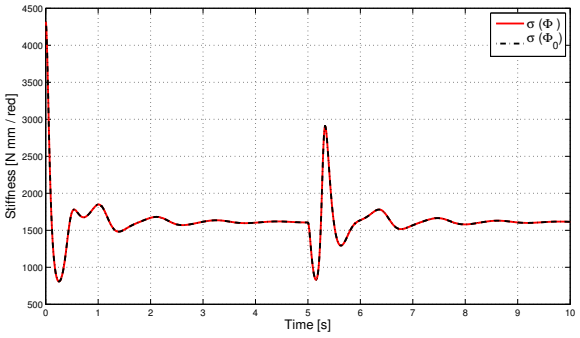

(b)

Figure 10: Comparison of link position (a) and device stiffness (b) for the VSA-II without gravity [dot-dashed, black], and with gravity under the dynamic cancellation law [continuous, red] when the bang-bang torque inputs τ_{10} and τ_{10} of Fig. 7(c) are applied

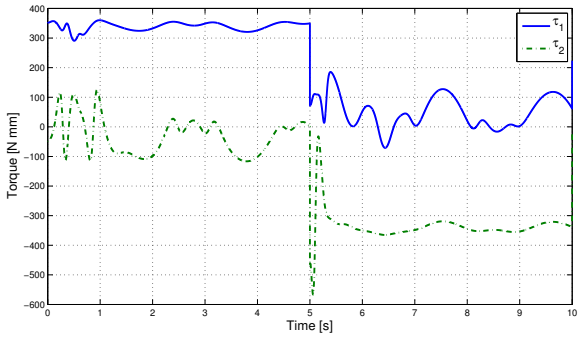

Figure 11: Total applied torques for the link motion and device stiffness evolution of Fig. 10

where K is the constant stiffness of each of the two torsional elastic springs and

$$\beta(\phi_i) = \arcsin\left(C \sin\left(\frac{\phi_i}{2}\right)\right) - \frac{\phi_i}{2}, \qquad i = 1, 2,$$

being $C > 1$ a geometric parameter of the 4-bar mechanisms. Due to this arrangement, the dynamic gravity cancellation law for the VSA-II is a particular instance of eq. (39).

Figure 10 shows the obtained evolution when using the same open-loop torque input of Fig. 7(c) and the numerical data from [16, 21]. The total applied torques are reported in Fig. 11.

6 Antagonistic Actuation with Constant but Different Stiffness

As a particular case of the previous section, and still focusing on a single dof for simplicity, we consider here the antagonistic arrangement of two motors at the joint with transmissions having constant stiffness. However, we relax the symmetry assumption made in (31–33) and allow for possibly different stiffness of the two transmissions, as well as for different motor inertias and viscous coefficients on each motor side. Therefore, we have the *elastic* torques

$$\tau_{ei}(\phi_i) = K_i\phi_i = K_i(q - \theta_i), \qquad i = 1, 2,$$

and *constant* (but typically *different*) stiffnesses

$$\sigma_i = \frac{\partial \tau_{ei}(\phi_i)}{\partial q} = K_i, \qquad i = 1, 2.$$

The dynamic model is

$$M\ddot{q} + D_q\dot{q} + g(q) + K_1(q - \theta_1) + K_2(q - \theta_2) = 0 \tag{44}$$

$$B_1\ddot{\theta}_1 + D_{\theta_1}\dot{\theta}_1 + K_1(\theta_1 - q) = \tau_1 \tag{45}$$

$$B_2\ddot{\theta}_2 + D_{\theta_2}\dot{\theta}_2 + K_2(\theta_2 - q) = \tau_2. \tag{46}$$

The control goal is again to design a dynamic gravity cancellation feedback law so that the behavior of selected outputs of the gravity-loaded system (44–46) matches that associated to the gravity-free model. However, the procedure in Sect. 5 cannot be used as such here. In fact, the total device stiffness is now constant,

$$\sigma_t = K_1 + K_2, \tag{47}$$

and cannot be used as a linearizing coordinate (and, of course, it cannot be changed either). Therefore, the two motors provide *actuation redundancy* in this case. This redundancy will be used to define how the dynamic gravity load should be shared between the two motors and transmissions. The solution can be derived again within a feedback equivalence approach.

Before proceeding, the *static conditions* are analyzed with some detail. At any forced equilibrium configuration $(\bar{q}, \bar{\theta}_1, \bar{\theta}_2)$, with $\dot{q} = \ddot{q} = 0$ and $\dot{\theta}_i = \ddot{\theta}_i = 0$, $i = 1, 2$, the following relations hold:

$$\begin{aligned} g(\bar{q}) + K_1(\bar{q} - \bar{\theta}_1) + K_2(\bar{q} - \bar{\theta}_2) &= 0 \\ K_1(\bar{\theta}_1 - \bar{q}) &= \bar{\tau}_1 \\ K_2(\bar{\theta}_2 - \bar{q}) &= \bar{\tau}_2. \end{aligned}$$

Adding them up, it follows that $\bar{\tau}_1 + \bar{\tau}_2 = g(\bar{q})$. To resolve this linear constraint in terms of the single static motor torques $\bar{\tau}_1$ and $\bar{\tau}_2$, one can minimize a weighted quadratic function

$$H = \frac{1}{2}\left(w_1\bar{\tau}_1^2 + w_2\bar{\tau}_2^2\right), \qquad w_i > 0,\ i = 1, 2.$$

The solution is

$$\bar{\tau}_1 = \frac{w_2}{w_1 + w_2}\, g(\bar{q}), \qquad \bar{\tau}_2 = \frac{w_1}{w_1 + w_2}\, g(\bar{q}). \tag{48}$$

While the positive weights w_1 and w_2 can be chosen in principle in an arbitrary way, a relevant case is obtained by selecting the *transmission compliances* as weights, since the system will then satisfy an intrinsic physical property.

In fact, for any value $\bar{q}$ and any set of static torques satisfying $\bar{\tau}_1 + \bar{\tau}_2 = g(\bar{q})$, the natural equilibrium of the motor positions $\bar{\theta}_1$ and $\bar{\theta}_2$ is found by minimizing the total elastic potential:

$$\begin{aligned} &\min\ U_e = \tfrac{1}{2}\left(K_1(\theta_1 - \bar{q})^2 + K_2(\theta_2 - \bar{q})^2\right) \\ &\text{subject to} \quad K_1(\theta_1 - \bar{q}) + K_2(\theta_2 - \bar{q}) = g(\bar{q}). \end{aligned}$$

The unique solution is given by $\bar{\theta}_i = \bar{q} + g(\bar{q})/(K_1 + K_2)$, $i = 1, 2$, and provides

$$\bar{\tau}_1 = \frac{K_1}{K_1 + K_2}\, g(\bar{q}), \qquad \bar{\tau}_2 = \frac{K_2}{K_1 + K_2}\, g(\bar{q}). \tag{49}$$

The two equations in (49) are in the form (48), with weights chosen as the compliances $w_1 = 1/K_1$ and $w_2 = 1/K_2$. Therefore, the motor with the stiffer transmission will carry the larger part of the static gravity load. In the limit, when, e.g., $K_1 \to \infty$, we will have $\bar{\tau}_{1,\infty} = g(\bar{q})$, $\bar{\tau}_{2,\infty} = 0$.

Turning to *dynamic conditions*, we define next an auxiliary output function y that can be used as part of the linearizing coordinate transformation. Motivated by the fact that the total flexibility torque $\tau_{e1} + \tau_{e2}$ is a linear function of θ_1 and θ_2, we choose

$$y = \alpha_1\theta_1 + \alpha_2\theta_2, \tag{50}$$

with arbitrary constants α_i, $i = 1, 2$. Differentiating (44) and (50) twice, and using eqs. (45–46) and (47), yields

$$\begin{aligned} Mq^{[4]} + D_q q^{[3]} + \ddot{g}(q) + \sigma_t \ddot{q} &= K_1\ddot{\theta}_1 + K_2\ddot{\theta}_2 \\ &= \begin{pmatrix} \dfrac{K_1}{B_1} & \dfrac{K_2}{B_2} \end{pmatrix} \begin{pmatrix} \tau_1 + K_1(q - \theta_1) - D_{\theta_1}\dot{\theta}_1 \\ \tau_2 + K_2(q - \theta_2) - D_{\theta_2}\dot{\theta}_2 \end{pmatrix} \end{aligned} \tag{51}$$

and

$$\begin{aligned} \ddot{y} &= \alpha_1\ddot{\theta}_1 + \alpha_2\ddot{\theta}_2 \\ &= \begin{pmatrix} \dfrac{\alpha_1}{B_1} & \dfrac{\alpha_2}{B_2} \end{pmatrix} \begin{pmatrix} \tau_1 + K_1(q - \theta_1) - D_{\theta_1}\dot{\theta}_1 \\ \tau_2 + K_2(q - \theta_2) - D_{\theta_2}\dot{\theta}_2 \end{pmatrix}. \end{aligned} \tag{52}$$

The decoupling matrix associated to (Mq, y),

$$\boldsymbol{\mathcal{A}} = \begin{pmatrix} K_1 & K_2 \\ \alpha_1 & \alpha_2 \end{pmatrix} \begin{pmatrix} \frac{1}{B_1} & 0 \\ 0 & \frac{1}{B_2} \end{pmatrix}, \tag{53}$$

is now constant, and nonsingular iff $K_1\alpha_2 - K_2\alpha_1 \neq 0$. In particular, this is certainly true for $\alpha_1\alpha_2 < 0$, as well as when only one of the α_i's is zero. Indeed, the first block matrix in $\boldsymbol{\mathcal{A}}$ appears also in the change of state coordinates between $(q, \theta_1, \theta_2, \dot{q}, \dot{\theta}_1, \dot{\theta}_2)$ and $(q, \dot{q}, \ddot{q}, q^{[3]}, y, \dot{y})$ and its nonsingularity makes this a globally invertible map.

At this stage, we can repeat the same calculations for the gravity-free system (where variables have a 0 subscript) and impose $q(t) \equiv q_0(t)$ and $y(t) \equiv y_0(t)$ for all $t \geq 0$. Following the same line of thoughts of the previous sections, comparison of expressions (51) and (52) of the gravity-loaded system with those of the gravity-free case yields, after some manipulation, the dynamic gravity cancellation law

$$\begin{pmatrix} \tau_1 \\ \tau_2 \end{pmatrix} = \begin{pmatrix} \tau_{10} \\ \tau_{20} \end{pmatrix} + \begin{pmatrix} \tau_{1g} \\ \tau_{2g} \end{pmatrix} \tag{54}$$

where

$$\begin{aligned}\tau_{1g} &= \frac{\alpha_2}{K_1\alpha_2 - K_2\alpha_1}\big(K_1 g(q) + D_{\theta_1}\dot{g}(q) + B_1\ddot{g}(q)\big)\\ \tau_{2g} &= \frac{-\alpha_1}{K_1\alpha_2 - K_2\alpha_1}\big(K_2 g(q) + D_{\theta_2}\dot{g}(q) + B_2\ddot{g}(q)\big)\end{aligned} \tag{55}$$

and τ_{i0}, $i = 1, 2$ are the control commands designed in the absence of gravity. Note that (54–55) can be seen as a simpler (and more explicit) form of eq. (39), obtained by replacing $\sigma_t(\phi_1, \phi_2)$ with y and taking into account the fact that the device stiffness and the $\boldsymbol{\mathcal{A}}$ matrix are constant. The above closed-form control expression is obtained without the need for a numerical search, similarly to the case of constant elastic joints with single actuation considered in Sect. 2.

The control expressions (55) contain the arbitrary design parameters α_1 and α_2. As such, they can be view as the general solution to the problem of sharing dynamic gravity cancellation between the two motors of the antagonistic joint. In particular, wishing to use only one motor for gravity cancellation, e.g., the first one, we set $\alpha_1 = 0$ (with any $\alpha_2 \neq 0$) obtaining $\tau_{2g} = 0$ and

$$\tau_{1g} = g(q) + \frac{D_{\theta_1}}{K_1}\,\dot{g}(q, \dot{q}) + \frac{B_1}{K_1}\,\ddot{g}(q).$$

This is exactly the scalar version of eq. (13) in Sect. 2. On the other hand, by setting $\alpha_1 = -1$ and $\alpha_2 = 1$ we obtain a dynamic sharing of gravity that, in static conditions, collapses into the associated natural optimum (49). Note also that when $K_1 = K_2$, the only forbidden choice is $\alpha_1 = \alpha_2$. Furthermore, it is easy to realize that the output structure (50) could be generalized to

$$y = \alpha_1(q, \dot{q})\theta_1 + \alpha_2(q, \dot{q})\theta_1$$

without any major changes in the derivations. Provided that invertibility of the decoupling matrix $\boldsymbol{\mathcal{A}}$ is enforced (this matrix would have the same structure of (53), but depending then on $(q, \dot{q})$), such output structure may allow for a state-dependent, and possibly optimal, dynamic sharing.

Note finally that, if m motors were connected in parallel to the link through m transmissions of constant (and different) stiffnesses and we were using a combination of motors to cancel gravity from the link motion, the solution would take the form

$$\tau_{ig} = \frac{\alpha_i}{K_i\alpha_i - \sum\limits_{\substack{j=1\\ j\neq i}}^{m} K_j\alpha_j}\big(K_i g(q) + D_{\theta_i}\dot{g}(q) + B_i\ddot{g}(q)\big), \tag{56}$$

with α_i being the discounting factor of the i-th motor, for $i = 1, \ldots, m$.

All developments in this section can be replicated in a straightforward way for the case of n-dof robots with antagonistic actuation at all joints, each with two (different or equal) constant stiffnesses.

6.1 Simulation results

We tested the control law (54–55) for a single link with an antagonistic elastic joint having the two transmissions, respectively, of stiffness $K_1 = 100$ and $K_2 = 50$ [N·mm/rad], and thus with a constant $\sigma_t = 150$ [N·mm/rad]. The other numerical data are the same of Sect. 2.1, duplicated as needed. Two equal open-loop sinusoidal torques $\tau_{10} = \tau_{20} = \sin 2\pi t$ were applied for $T = 10$ s, see Fig. 13(c). Choosing $\alpha_1 = \alpha_2 = 0.5$, the results of Fig. 12 indicate full agreement with the theory. The total torques applied by the two motors are shown in Fig. 13(a),(b). For comparison, we report also the motor evolutions for two other choices of the output constants in the same previous operative conditions. Figure 14 refers to the case $\alpha_1 = 0$ and $\alpha_2 = 2$, where the first motor is fully responsible for canceling the gravity torque. Figure 15 refers to the choice $\alpha_1 = -1$ and $\alpha_2 = 1$. In this case, the smallest global deviations from the unloaded case are obtained, indicating a potential condition of optimal dynamic sharing of gravity. Indeed, in all previous situations the link motion replicates the no-gravity behavior.

7 Conclusions

We have considered the problem of perfect cancellation of dynamic gravity effects acting on the link motion of robot manipulators having flexible transmissions. The cases of flexible transmissions having constant or nonlinear stiffness characteristics with single actuation at each joint, and of variable nonlinear or constant stiffness with (double) antagonistic actuation have been analyzed. Based on the feedback equivalence principle, nonlinear control laws have been designed that allow the outputs of the gravity-loaded to behave as those of a reference model where gravity is absent. In the case of VSA-based manipulators, this includes the dynamic shaping of both the link motion and the evolution of the device stiffness. For double antagonistic actuation with constant stiffness, an actuation redundancy occurs and gravity load sharing among the motors can be optimized in static or dynamic terms.

Dynamic gravity cancellation involves in general the on-line computation of inertial terms, but the presented control laws are still much simpler than those needed for feedback linearization. The control laws solving the problem have been obtained either in closed algebraic form or by using simple numerical techniques. In particular, a parallel simulation of the gravity-free system to be matched is never required.

The presented results can be used for different control purposes. For set-point regulation tasks, a PD-type state feedback law has been designed on top of the gravity cancellation law in the case of robots with elastic joints. Global asymptotic stability has been shown using Lyapunov techniques, without the need of a strictly positive lower bound neither on the proportional gain nor on the joint stiffness. In a similar way, we foresee that enhanced regulation controllers could be obtained with

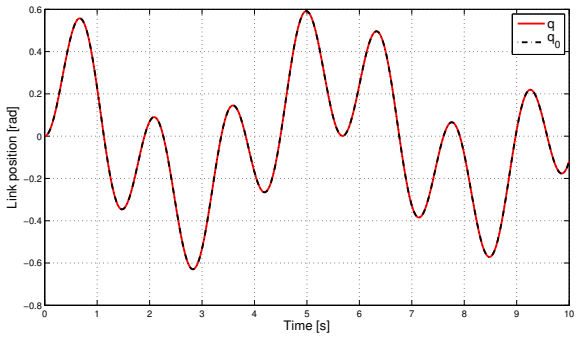

(a)

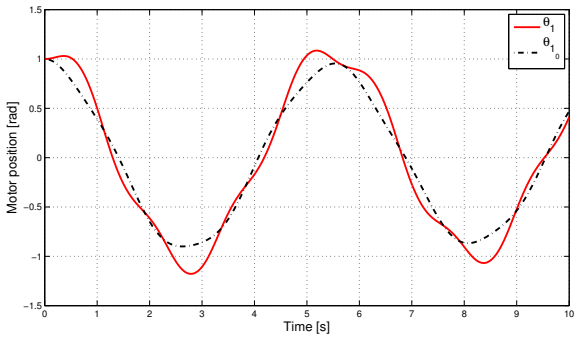

(b)

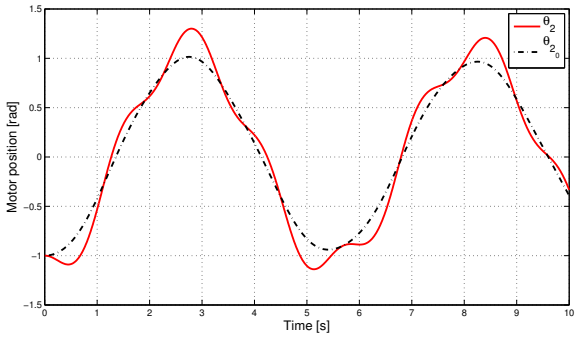

(c)

Figure 12: Comparison of the position of the link (a) and of the two motors (b,c) for the antagonistic joint arrangement having different but constant stiffnesses without gravity [dot-dashed, black], and with gravity under the dynamic cancellation law (54–55) [continuous, red]; the output coefficients in (50) are $\alpha_1 = \alpha_2 = 0.5$

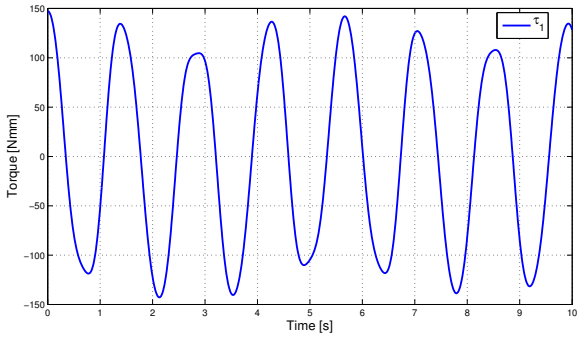

(a)

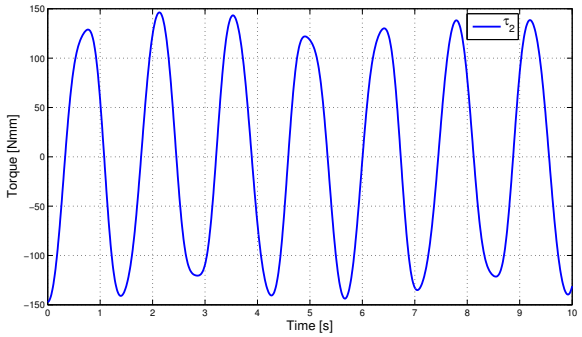

(b)

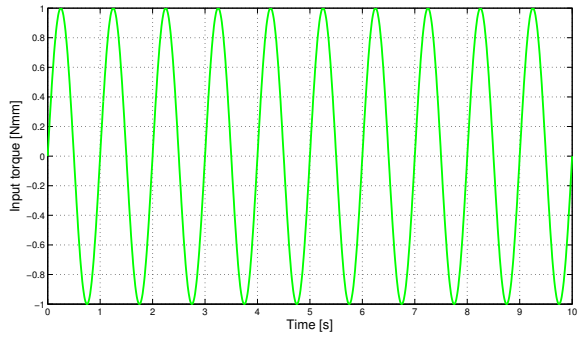

(c)

Figure 13: Total applied torques by the first (a) and second (b) motor for the link motion of Fig. 12 when the sinusoidal open-loop torques $\tau_{10} = \tau_{20}$ (c) are commanded

relative ease also for VSA-based manipulators, where the link position as well as the device stiffness need to be asymptotically stabilized to a desired constant value.

The proposed dynamic gravity cancellation is also useful in safe physical human-

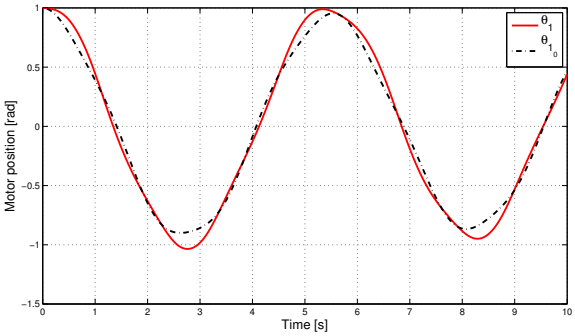

(a)

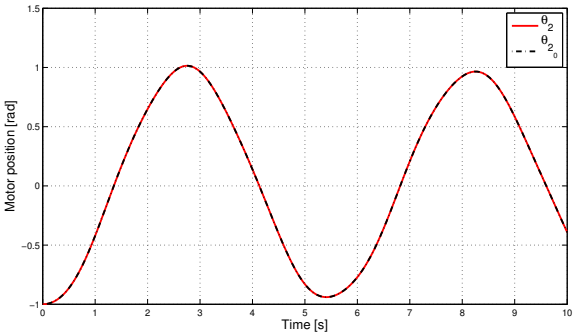

(b)

Figure 14: Comparison of the first (a) and second (b) motor positions for the antagonistic joint arrangement having different but constant stiffnesses without gravity [dot-dashed, black], and with gravity under the dynamic cancellation law (54–55) [continuous, red]; the output coefficients in (50) are $\alpha_1 = 0$ and $\alpha_2 = 2$

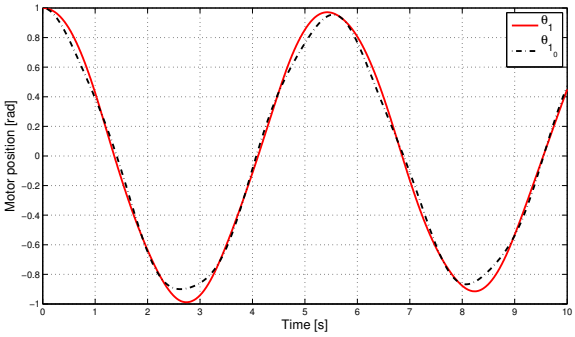

(a)

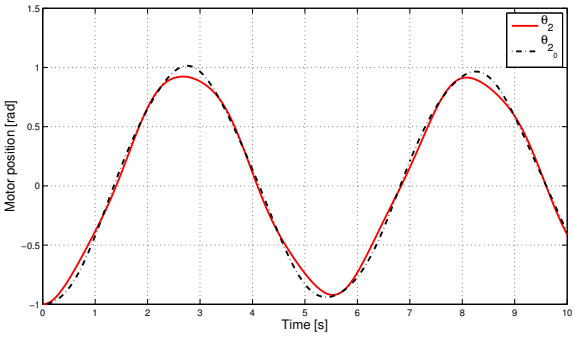

(b)

Figure 15: Comparison of the first (a) and second (b) motor positions for the antagonistic joint arrangement having different but constant stiffnesses without gravity [dot-dashed, black], and with gravity under the dynamic cancellation law (54–55) [continuous, red]; the output coefficients in (50) are $\alpha_1 = -1$ and $\alpha_2 = 1$

robot interaction. In general, unexpected collisions may occur at any time during motion and the compliant robot should react as soon as the impact is detected (e.g., with a sensorless residual-based method as in [2]). Through the permanent cancellation of the gravitational loads on the robot links, a physical torque-based reaction strategy can be designed so that the controlled robot rapidly flees away from the danger area in a gravity-unbiased dynamic fashion. This subject is currently under investigation.

Acknowledgments

This work has been funded by the MIUR project PRIN 2007 SICURA.

References

[1] J. Heinzmann and A. Zelinsky, "Quantitative safety guarantees for physical human-robot interaction," *Int. J. of Robotics Research*, vol. 22, no. 7/8, pp. 479–504, 2003.

[2] A. De Luca, A. Albu-Schäffer, S. Haddadin, and G. Hirzinger, "Collision detection and safe reaction with the DLR-III lightweight robot arm," in *Proc. IEEE/RSJ Int. Conf. on Intelligent Robots and Systems*, 2006, pp. 1623–1630.

[3] A. De Santis, B. Siciliano, A. De Luca, and A. Bicchi, "An atlas of physical human-robot interaction," *Mechanism and Machine Theory*, vol. 43, no. 3, pp. 253–270, 2008.

[4] G. Hirzinger, A. Albu-Schäffer, M. Hähnle, I. Schaefer, and N. Sporer, "On a new generation of torque controlled light-weight robots," in *Proc. IEEE Int. Conf. on Robotics and Automation*, 2001, pp. 3356–3363.

[5] A. Bicchi and G. Tonietti, "Fast and soft arm tactics: Dealing with the safety-performance trade-off in robot arms design and control," *IEEE Robotics and Automation Mag.*, vol. 11, no. 2, pp. 22–33, 2004.

[6] A. De Luca and W. Book, "Robots with flexible elements," in *Handbook of Robotics*, B. Siciliano and O. Khatib, Eds., Springer, 2008, pp. 287–319.

[7] P. Tomei, "A simple PD controller for robots with elastic joints," *IEEE Trans. on Automatic Control*, vol. 36, no. 10, pp. 1208–1213, 1991.

[8] A. De Luca, B. Siciliano, and L. Zollo, "PD control with on-line gravity compensation for robots with elastic joints: Theory and experiments," *Automatica*, vol. 41, no. 10, pp. 1809–1819, 2005.

[9] A. Kugi, C. Ott, A. Albu-Schäffer, and G. Hirzinger, "On the passivity-based impedance control of flexible joint robots," *IEEE Trans. on Robotics*, vol. 24, no. 2, pp. 416 –429, 2008.

[10] S. Haddadin, A. Albu-Schäffer, A. De Luca, and G. Hirzinger, "Collision detection and reaction: A contribution to safe physical human-robot interaction," in *Proc. IEEE/RSJ Int. Conf. on Intelligent Robots and Systems*, 2008, pp. 3356–3363.

[11] M. W. Spong, "Modeling and control of elastic joint robots," *ASME J. of Dynamic Systems, Measurement, and Control*, vol. 109, no. 4, pp. 310–319, 1987.

[12] A. De Luca and P. Lucibello, "A general algorithm for dynamic feedback linearization of robots with elastic joints," in *Proc. IEEE Int. Conf. on Robotics and Automation*, 1998, pp. 504–510.

[13] A. Bicchi, S. L. Rizzini, and G. Tonietti, "Compliant design for intrinsic safety: General issue and preliminary design," in *Proc. IEEE/RSJ Int. Conf. on Intelligent Robots and Systems*, 2001, pp. 1864–1869.

[14] M. Zinn, O. Khatib, B. Roth, and J. K. Salisbury, "A new actuation approach for human-friendly robot design," *Int. J. of Robotics Research*, vol. 23, no. 4/5, pp. 379–398, 2005.

[15] S. A. Migliore, E. A. Brown, and S. P. DeWeerth, "Biologically inspired joint stiffness control," in *Proc. IEEE Int. Conf. on Robotics and Automation*, 2005, pp. 4508–4513.

[16] R. Schiavi, G. Grioli, S. Sen, and A. Bicchi, "VSA-II: A novel prototype of variable stiffness actuator for safe and performing robots interacting with humans," in *Proc. IEEE Int. Conf. on Robotics and Automation*, 2008, pp. 2171–2176.

[17] G. Boccadamo, R. Schiavi, S. Sen, G. Tonietti, and A. Bicchi, "Optimization and fail-safety analysis of antagonistic actuation for pHRI," in *European Robotics Symp.*, Springer Tracts in Advanced Robotics, Springer Berlin, 2006, pp. 109–118.

[18] S. Wolf and G. Hirzinger, "A new variable stiffness design: Matching requirements of the next robot generation," in *Proc. IEEE Int. Conf. on Robotics and Automation*, 2008, pp. 1741–1746.

[19] J. Choi, S. Park, W. Lee, and S.-C. Kang, "Design of a robot joint with variable stiffness," in *Proc. IEEE Int. Conf. on Robotics and Automation*, 2008, pp. 1760–1765.

[20] G. Palli, C. Melchiorri, and A. De Luca, "On the feedback linearization of robots with variable joint stiffness," in *Proc. IEEE Int. Conf. on Robotics and Automation*, 2008, pp. 1753–1759.

[21] A. De Luca, F. Flacco, A. Bicchi, and R. Schiavi, "Nonlinear decoupled motion-stiffness control and collision detection/reaction for the VSA-II variable stiffness device," in *Proc. IEEE/RSJ Int. Conf. on Intelligent Robots and Systems*, 2009, pp. 5487–5494.

[22] A. Isidori, *Nonlinear Control Systems*, 3rd ed., Springer, 1995.

[23] N. Kircanski and A. Goldenberg, "An experimental study of nonlinear stiffness, hysteresis, and friction effects in robot joints with harmonic drives and torque sensors," *Int. J. of Robotics Research*, vol. 16, no. 2, pp. 214–239, 1997.